Metal and Metal Oxide Nanoparticle Synthesis from Metal Organic Frameworks (MOFs): finding the border of Metal and Metal oxides

Raja Das, Pradip Pachfule, and Rahul Banerjee and Pankaj Poddar**

Physical & Materials Chemistry Division, National Chemical Laboratory, Dr. Homi Bhabha Road, Pune-411008

E-mail: p.poddar@ncl.res.in Fax: + 91-20-25902636; Tel: + 91-20-25902580
r.banerjee@ncl.res.in Fax: + 91-20-25902636; Tel: + 91-20-25902535

Supporting Information

Content

Section 1. Experimental measurements and methods used:

4,4'-(hexafluoroisopropylidene) bis(benzoic acid), $Co(NO_3)_2.6H_2O$ and $Mn(NO_3)_2.xH_2O$ were purchased from Aldrich Chemicals. 3-methyl pyridine and *N*, *N*-dimethylformamide (DMF) were purchased from Rankem chemicals. 1,3-Adamantanediacetic Acid, 4,4′-bipyridine, $Cd(NO_3)_2.4H_2O$, $Zn(NO_3)_2.6H_2O$ and $Cu(NO_3)_2.3H_2O$ were purchased from the Aldrich Chemicals. All starting materials were used without further purification. All experimental operations were performed in air and all the stock solutions were prepared in *N*, *N*-dimethylformamide (DMF).

PXRD, TGA and HRTEM Experiments: The X-ray diffraction patterns were recorded using PANalytical X'PERT PRO instrument using iron-filtered Cu Kα radiation (λ=1.5406 Å) in the 2θ range of 10°- 70° with a step size of 0.02° and a time of 0.3 second per step. Thermogravimetric (TGA) experiments were carried out in the temperature range of 20–900 °C on a SDT Q600 TG-DTA analyzer under N_2 and air atmosphere at a heating rate of 10 °C min^{-1}. To investigate the microstructure and morphology of the particles, we used the FEI (model Tecnai F30) high resolution transmission electron microscope (HRTEM) equipped with field emission source operating at 300 KV to image the nanocrystals on carbon-coated copper TEM grids. The nanoparticles were dispersed in ethanol and drop casted on the TEM grids.

Magnetic Measurements: All the magnetic measurements were done using a Physical Property Measurement System (PPMS) from Quantum Design Inc. San Diego, USA equipped with a 7 Tesla superconducting magnet and a vibrating sample magnetometer. The magnetic signal from the sample holder was negligible to affect our data accuracy. These measurements were carried out on polycrystalline samples. DC magnetization vs. T curves

were taken at 500 Oe field in field cooled (FC) and zero field cooled (ZFC) modes with heating/cooling rate of 2 K per minute. Magnetizations vs. field loops were taken in a field sweep from -50 kOe to +50 kOe at a rate of 75 Oe/sec.

Gas Adsorption Measurements: Low pressure volumetric gas adsorption measurements involved in this work were performed at 77 K for H_2 and N_2, maintained by a liquid nitrogen bath, with pressures ranging from 0 to 760 Torr on Quantachrome Quadrasorb automatic volumetric instrument. While CO_2 adsorption measurements were done at room temperature (298 K) with same pressures range. In the all adsorption measurements, ultra high-purity H_2 was obtained by using calcium aluminosilicate adsorbents to remove trace amounts of water and other impurities before introduction into the system. Samples were heated at 90 °C for 12 h and 150 °C for 12 h under a dynamic vacuum.

XPS and Raman Measurements: High resolution XPS data was collected by using a VG Microtch, model number ESCA 3000. The binding energy resolution was 0.1 eV. We used Shirley algorithm for background correction and chemically distinct species were resolved using a nonlinear least squares fitting procedure. The Raman spectra were recorded on a HR 800 Raman spectrophotometer (Jobin Yvon- Horiba, France) using monochromatic radiation emitted by a He-Ne laser (632.8 nm), operating at 20 mW.

Section 2. Detailed synthesis procedure, PXRD, TGA of *F*-MOF-4 and synthesis, properties of Cu/CuO nanoparticles:

$[Cu_2(hfbba)_2(3\text{-mepy})_2]$. $(DMF)_2(3\text{-mepy})$ (*F*-MOF-4) : 0.5 mL 3-methyl-pyridine stock solution (0.20 M) and 1.5 mL H2hfbba stock solution (0.20 M) in DMF were mixed in a 5 mL vial. To this solution was added 0.5 mL $Cu(NO_3)_2.3H_2O$ stock solution (0.20 M). The vial was capped and heated to 85 ^{O}C for 96 h. The mother liquor was decanted and the products were washed with DMF (15 mL) three times. Blue coloured crystals of *F*-MOF-4 were collected by filtration and dried in air (10 min) (yield: 50%; 0.0120 mg based on $Cu(NO_3)_2 \bullet 3H_2O$).

FT-IR: (KBr 4000-450cm-1): 3676 (br), 3068 (w), 3935 (m), 2657 (w), 2548 (w), 2331 (s), 1944 (m), 1816 (w), 1683 (m), 1632 (w), 1561 (w), 1410 (s), 1291 (w), 1239 (s), 1174 (w), 1090 (w), 1020 (w), 971 (w), 929 (w), 846 (m), 780 (s), 748 (w), 706 (w), 514 (m), 494 (w).

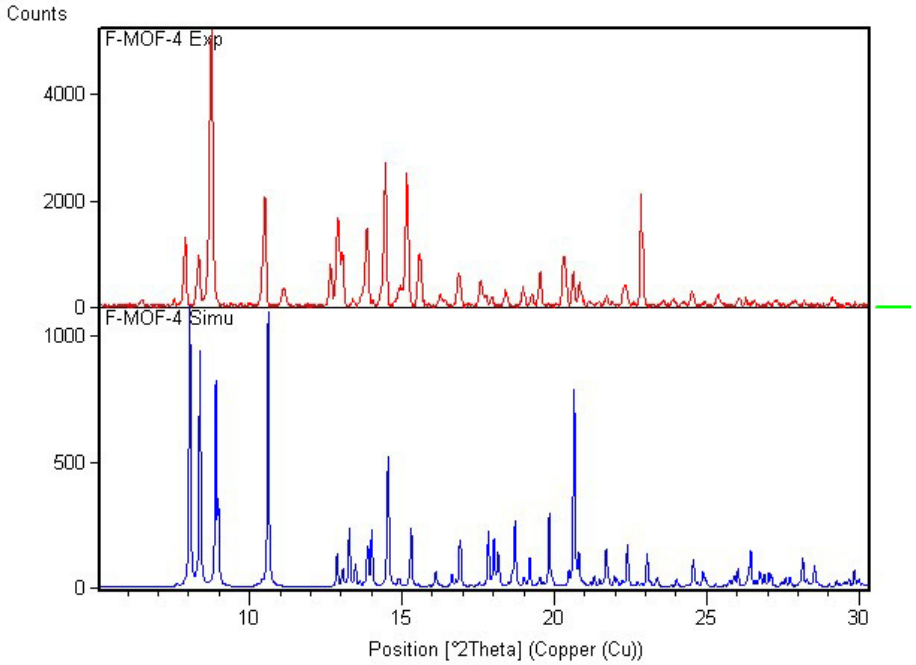

Figure 1: Comparison of the experimental PXRD pattern of as-synthesized FMOF-4 (top) with the one simulated from its single crystal structure (bottom).

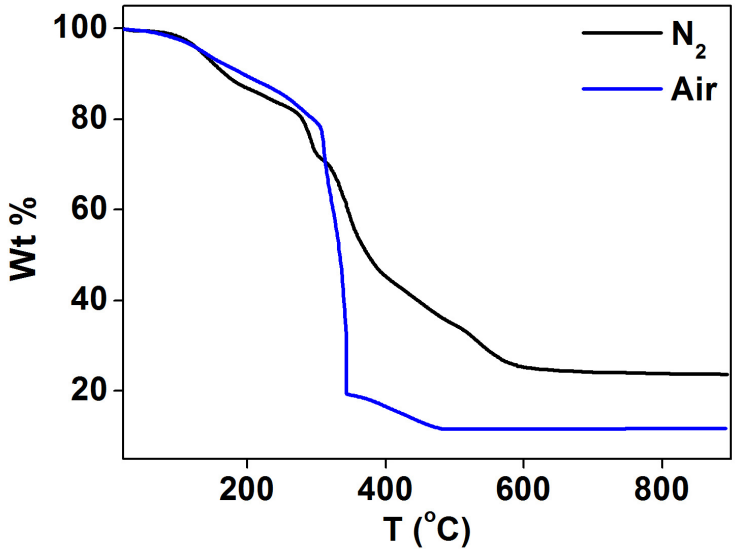

Figure S2: Thermal stability and the thermal gravimetric analysis (TGA) data of FMOF-4 in air and N_2 environment.

The as prepared $[Cu_2(hfbba)_2(3\text{-mepy})_2]\bullet(DMF)_2(3\text{-mepy})$ **(*F*-MOF-4)** was taken in a silica boat and then placed in a tube furnace and heated from room temperature to 900 ◦C under N_2 with a heating rate of 10 ◦C/min to thermolyze the organic species. After reaching the target temperature, the material was cool to room temperature. The final product was a black coloured powder.

The as prepared $[Cu_2(hfbba)_2(3\text{-mepy})_2]\bullet(DMF)_2(3\text{-mepy})$ **(*F*-MOF-4)** was taken in a silica boat and placed in a tube furnace and heated from room temperature to 900 °C under air with a heating rate of 10 ◦C/min to thromolyze the organic species. After reaching, 900 °C the material was cool to room temperature. The final product was a black coloured powder.

The TGA for ***F*-MOF-4** in air showed a gradual weight loss step of ~21% (20-300 °C), corresponding to escape of all N,N-dimethylformamide (DMF) in the pores followed by a

sharp weight loss ~60% (300-350 °C) probably due to the decomposition of the framework. Further ~8% weight loss (350-480 °C) could be due to crystallization process of CuO.

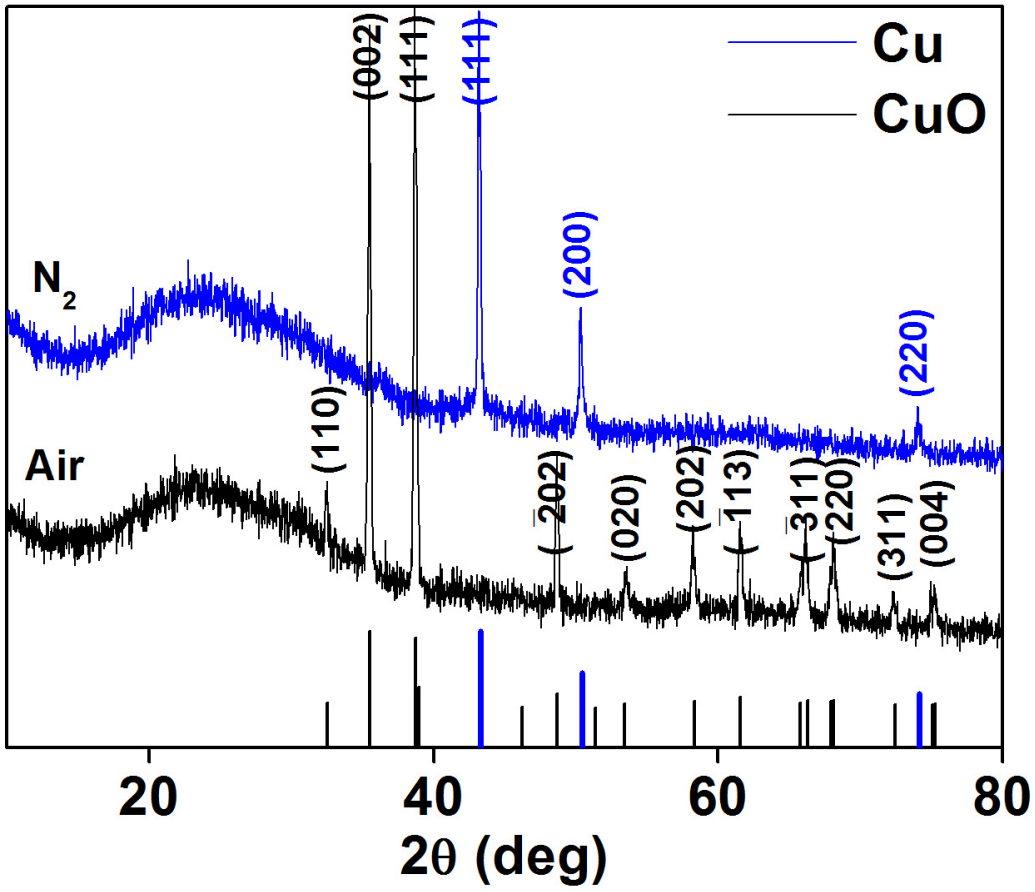

Figure S3. Powder x-ray diffraction patterns from a) JCPDS # 031005 data (red lines) for Cu and JCPDS # 450937 (black lines) data for CuO. b) CuO nanoparticles and c) Cu nanoparticles prepared by thermolysis of **(*F*-MOF-4)**. Background signal due to the presence of amorphous carbon can also be noticed.

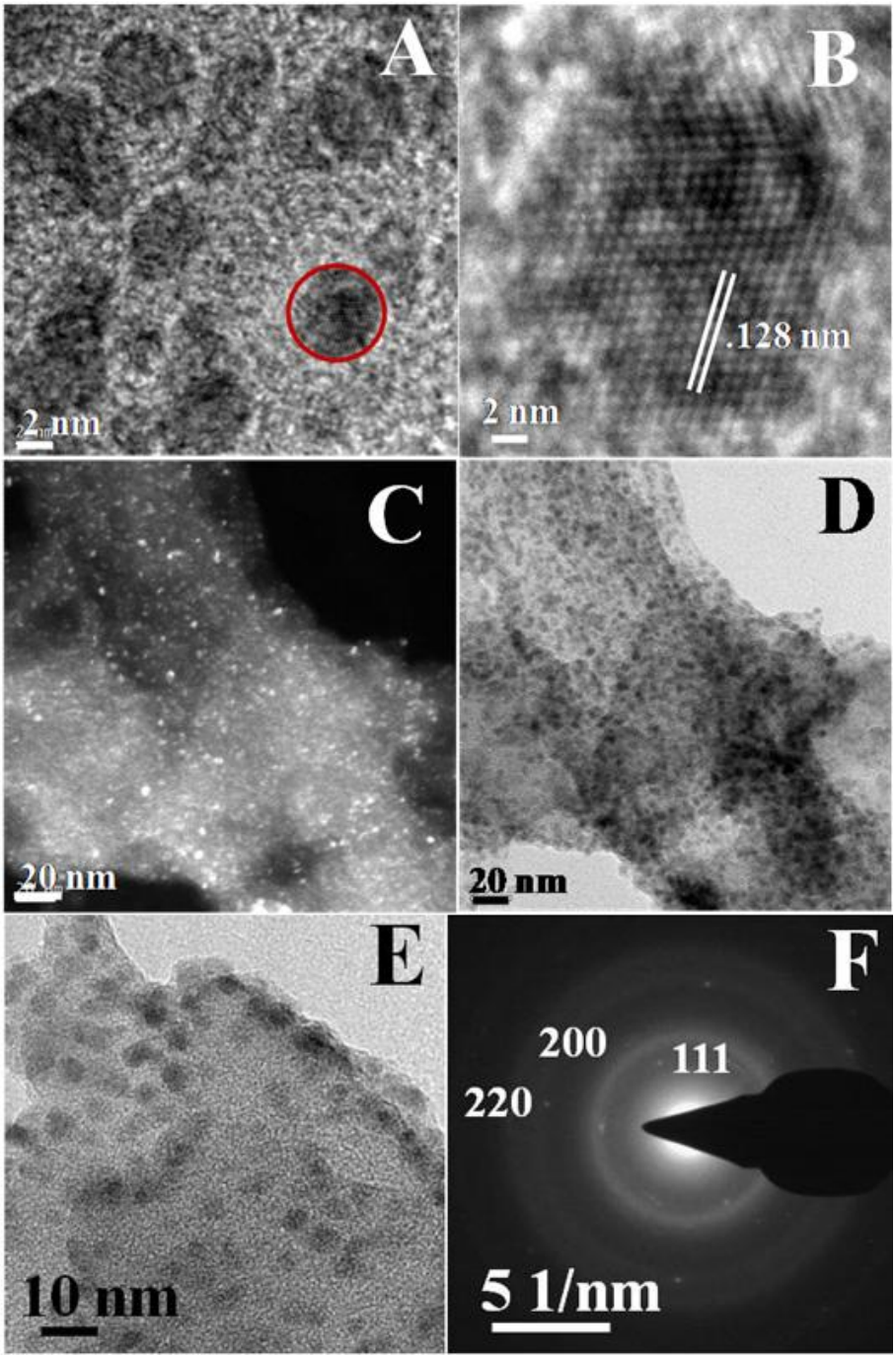

Figure S4: A) High-resolution TEM image B) A high-magnification lattice image of the circled portion of the image (A). C) Dark-field TEM image generated from the reflections in the electron diffraction pattern from the particles embedded in the carbon matrix showing the crystallinity of the particles. D) Corresponding bright-field image from the same portion. E) TEM image F) selected area electron diffraction (SAED) pattern of Cu nanoparticles prepared by thermolysis of **(*F*-MOF-4)**.

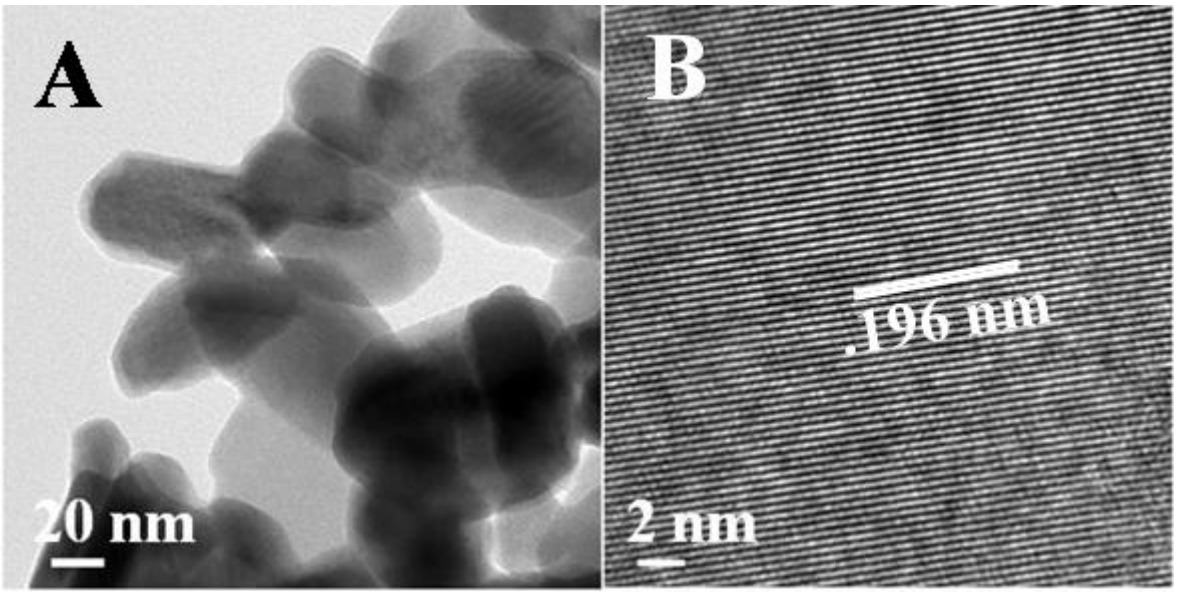

Figure S5: A) Transmission electron micrograph, B) high resolution TEM images showing the lattice fringes of CuO nanocrystals prepared by thermolysis of (***F*-MOF-4**) in air.

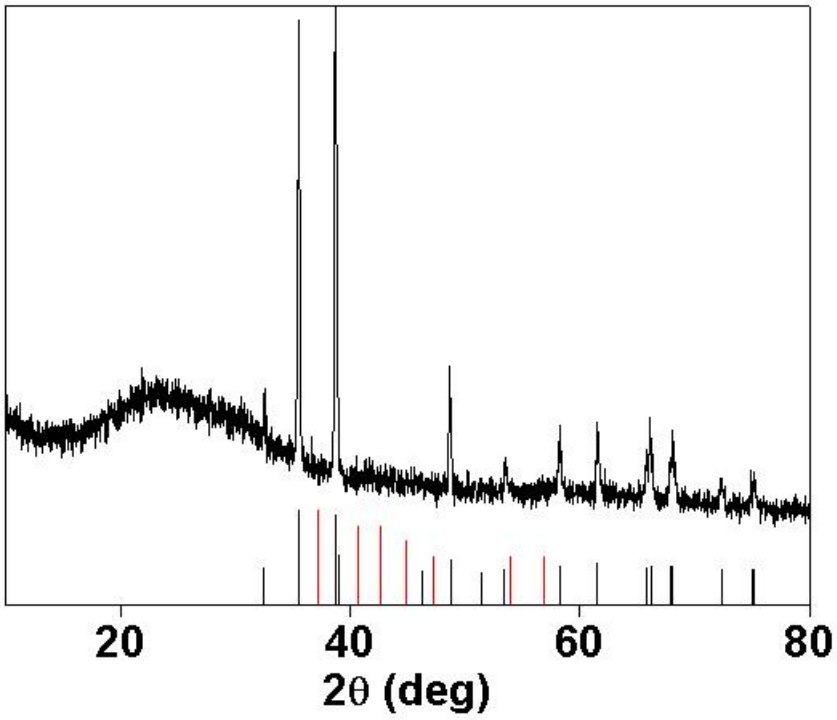

Figure S6: Powder x-ray diffraction patterns of CuO nanoparticles prepared by thermolysis of **(*F*-MOF-4)** and its comparison with JCPDS # 450937 (black line) for CuO and JCPDS # 351091 (red line) database for Cu_2O.

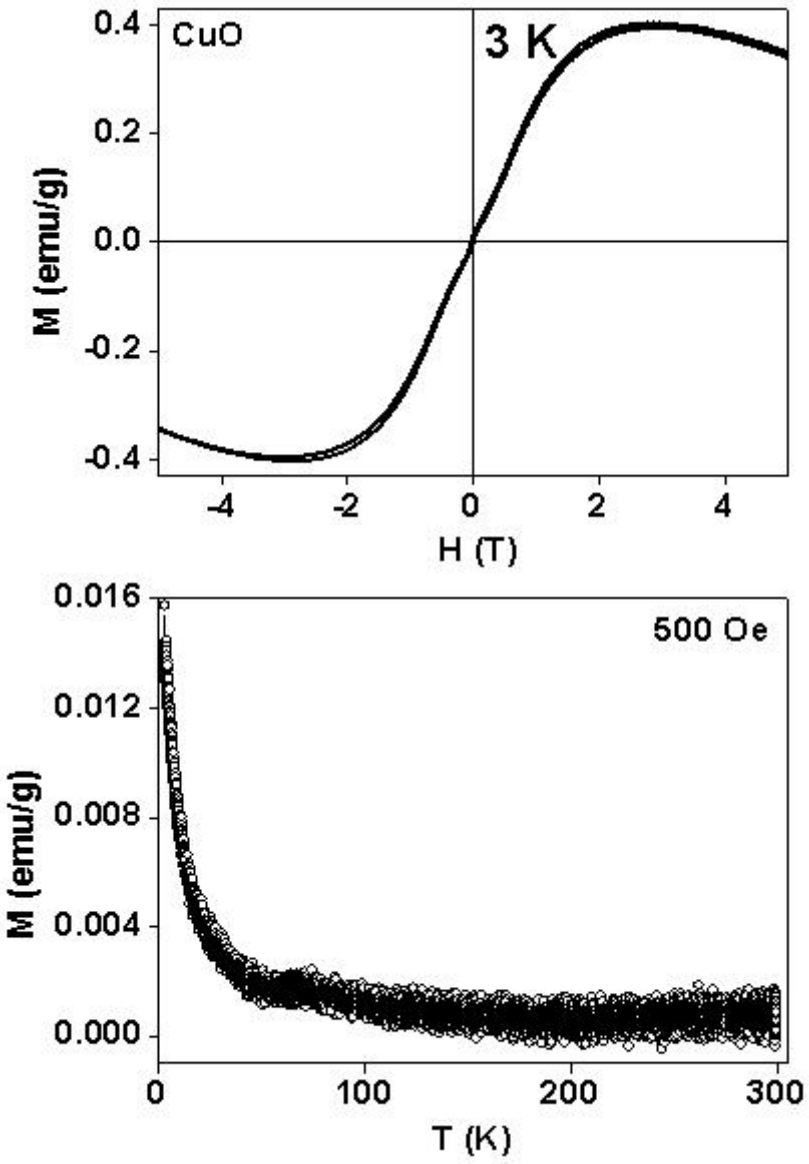

Figure S7: **(Top panel):** Hysteresis loop of CuO nanoparticles at 3 K **(Bottom panel):** Zero field cooled and field cooled curve of CuO nanoparticles prepared by thermolysis of **(*F*-MOF-4)** in air at 500 Oe external field.

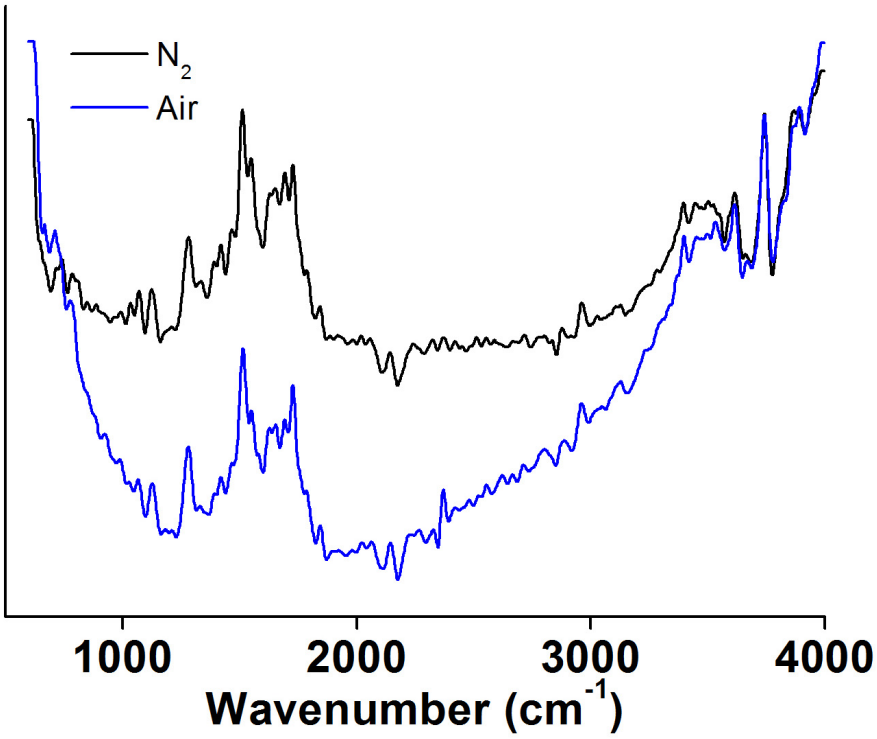

Figure S8: FTIR spectra of Cu and CuO nanoparticles prepared by thermolysis of **(*F*-MOF-4)**.

Section 3. Detailed synthesis procedure, PXRD, TGA of Co-H*F*MOF-D and synthesis, properties of Co/Co_3O_4 nanoparticles:

Synthesis of $[Co_2(hfbba)_2(3\text{-mepy})_2]\cdot(DMF)_3$ (Co-H*F*MOF-D) : 0.5 mL 3-methyl pyridine stock solution and 1.5 mL H_2hfbba stock solution (0.20 M) were mixed in a 5 mL vial. To this solution was added 0.5 mL $Co(NO_3)_2 \cdot 6H_2O$ stock solution (0.20 M). The vial was capped and heated to 85 °C for 96 h. The mother liquor was decanted and the products were washed with DMF (15 mL) three times. Dark pink colored crystals of Co-H*F*MOF-D were collected by filtration and dried in air (10 min) (Yield: 52%, 0.0151 gm depending on $Co(NO_3)_2 \cdot 6H_2O$).

FT-IR: **(KBr 4000-450cm-1):** 3393(m, br), 2935(w), 19441(w), 1628(m), 1406(s), 1172(s), 929(m), 780(m), 481(m) cm-1.

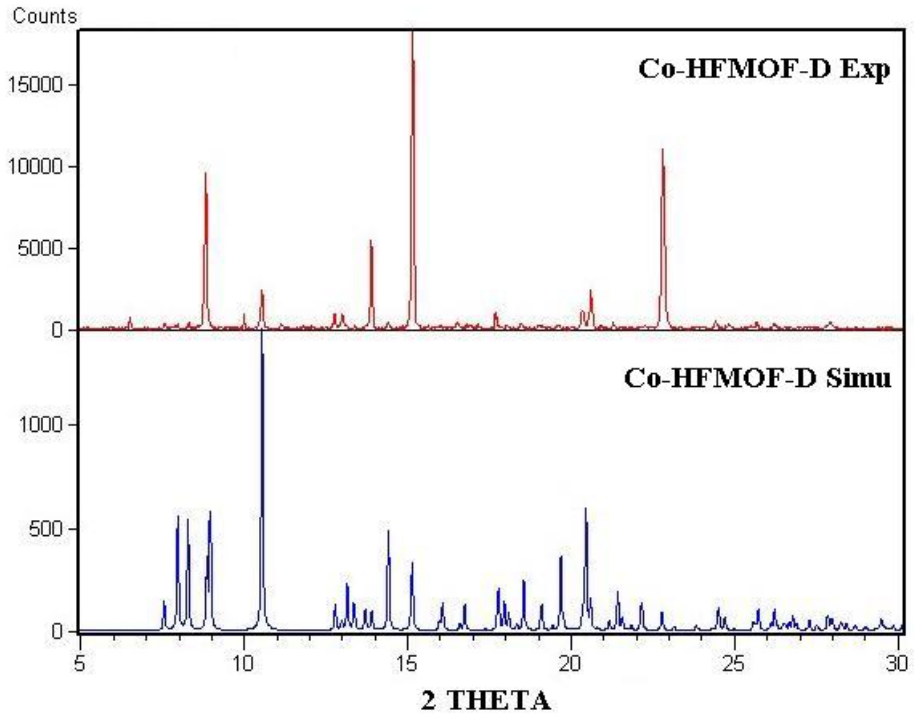

Figure S9: Comparison of the experimental PXRD pattern of as-synthesized **Co-H*F*MOF-D** (top) with the one simulated from its single crystal structure (bottom).

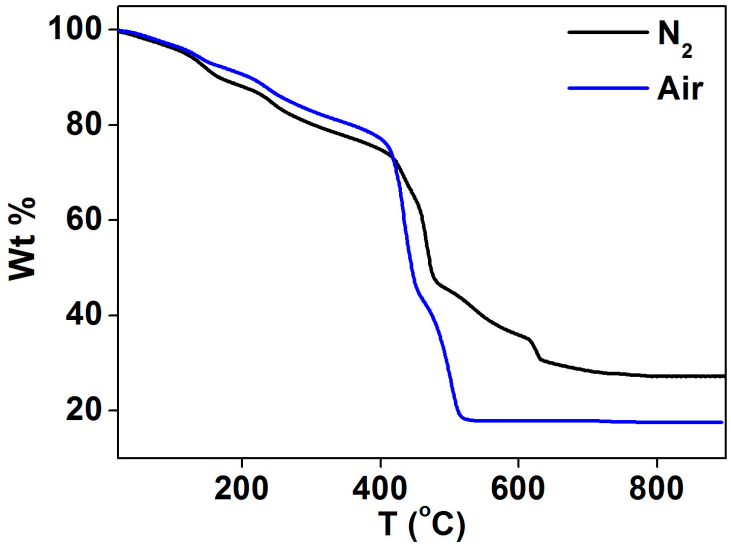

***Figure S10*:** Thermal stability and the thermal gravimetric analysis (TGA) data of **Co-H*F*MOF-D** in air and N_2 environment.

The as prepared $[Co_2(hfbba)_2(3\text{-mepy})_2]\bullet(DMF)_3$ (**Co-H*F*MOF-D**) was taken in a silica boat and then placed in a tube furnace and heated from room temperature to 900 ◦C under N_2 with a heating rate of 10 ◦C/min to thermolyze the organic species. After reaching the target temperature, the material was cool to room temperature. The final product was a black coloured powder.

The as prepared $[Co_2(hfbba)_2(3\text{-mepy})_2]\bullet(DMF)_3$ (**Co-H*F*MOF-D**) was taken in a silica boat and then placed in a tube furnace and heated from room temperature to 900 ◦C under air with a heating rate of 10 ◦C/min to thermolyzed the organic species. After reaching the target temperature, the material was cool to room temperature. The final product was a black coloured powder.

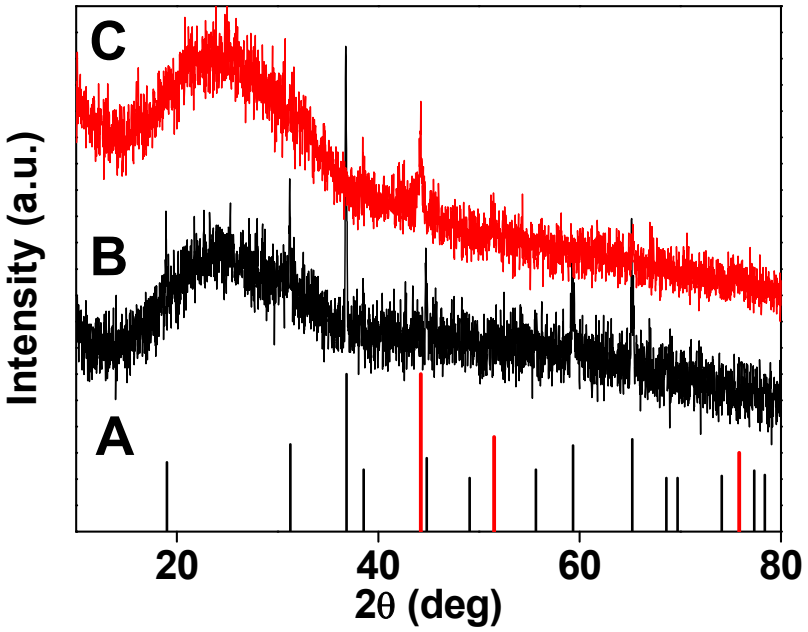

Figure S11: Powder x-ray diffraction patterns from the A) the JCPDS # 150806 data (red line) for Co and JCPDS # 431003(black lines) data for Co_3O_4. B) Co_3O_4 and C) Co nanoparticles prepared by thermolysis of (**Co-H*F*MOF-D**).

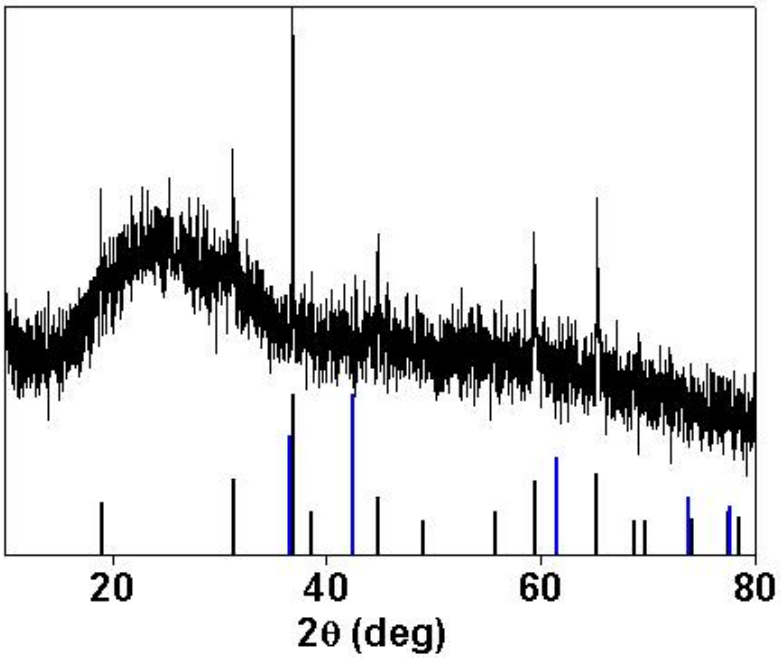

Figure S12: Powder x-ray diffraction patterns of Co_3O_4 nanoparticles prepared by thermolysis of **(Co-H*F*MOF-D)** and its comparison with JCPDS # 431003 (black line) for Co_3O_4 and JCPDS # 431004 (blue line) database for CoO.

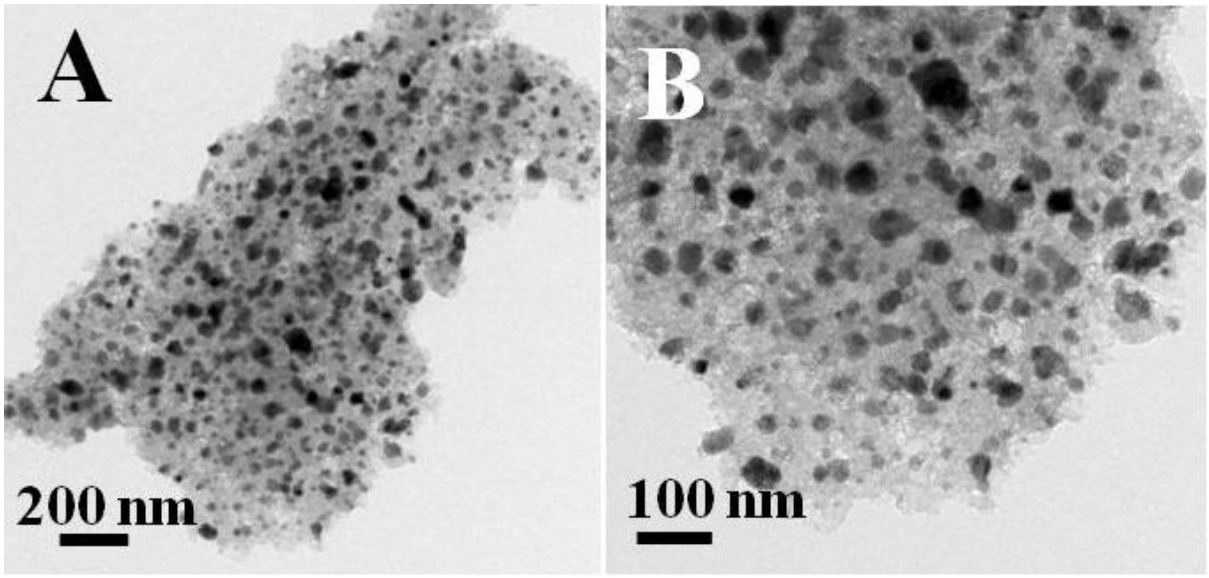

Figure S13: A,B) TEM images of Co nanoparticles prepared by thermolysis of **(Co-H*F*MOF-D).**

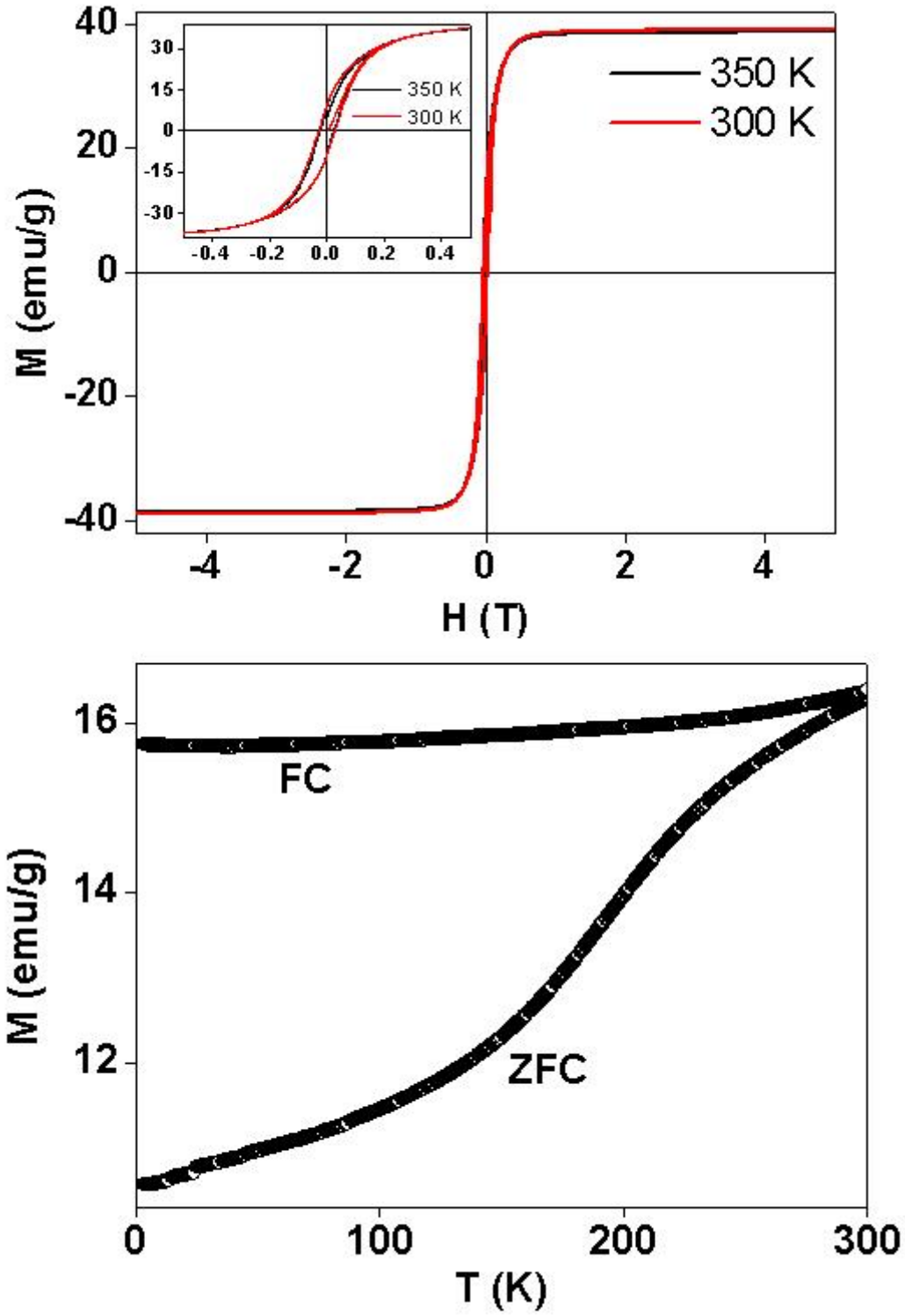

Figure S14: **(Top panel):** Hysteresis loop of cobalt nanoparticles at temperatures of 300 and 350 K (inset: hysteresis near zero field). **(Bottom panel):** Zero field cooled and field cooled curve of Co nanoparticles at 400 Oe external field.

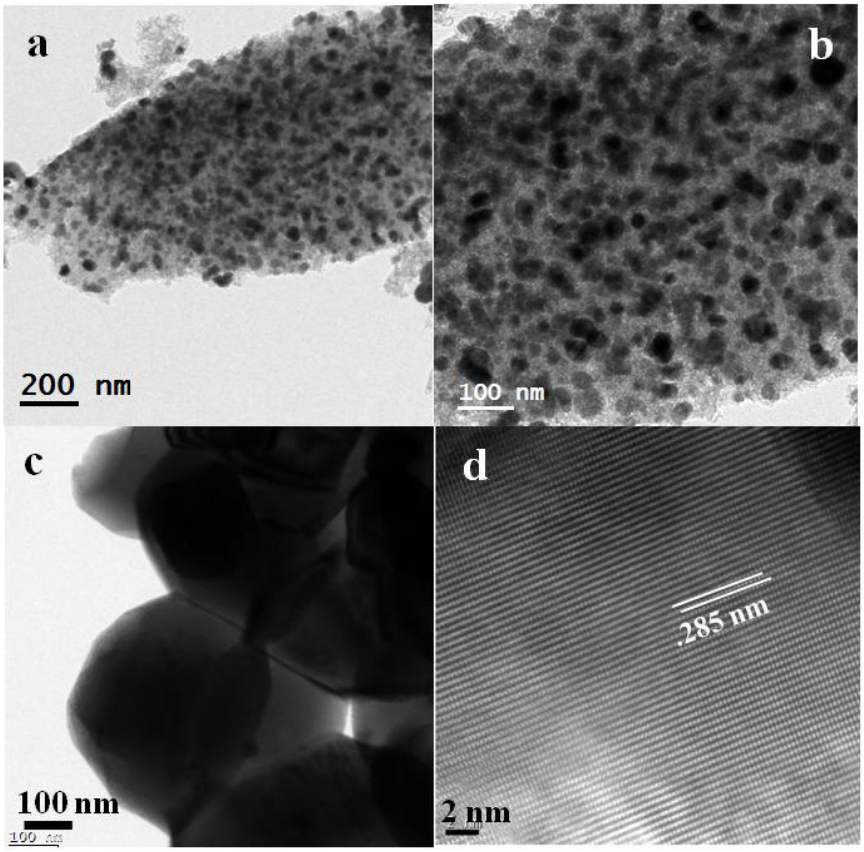

Figure S15: a-c) Transmission electron micrograph, d) high resolution TEM image showing the lattice fringes of Co_3O_4 nanocrystals prepared by thermolysis of (**Co-H*F*MOF-D**) in air. The *d*-values calculated from these images (shown in the nm scale) match with those obtained from powder XRD.

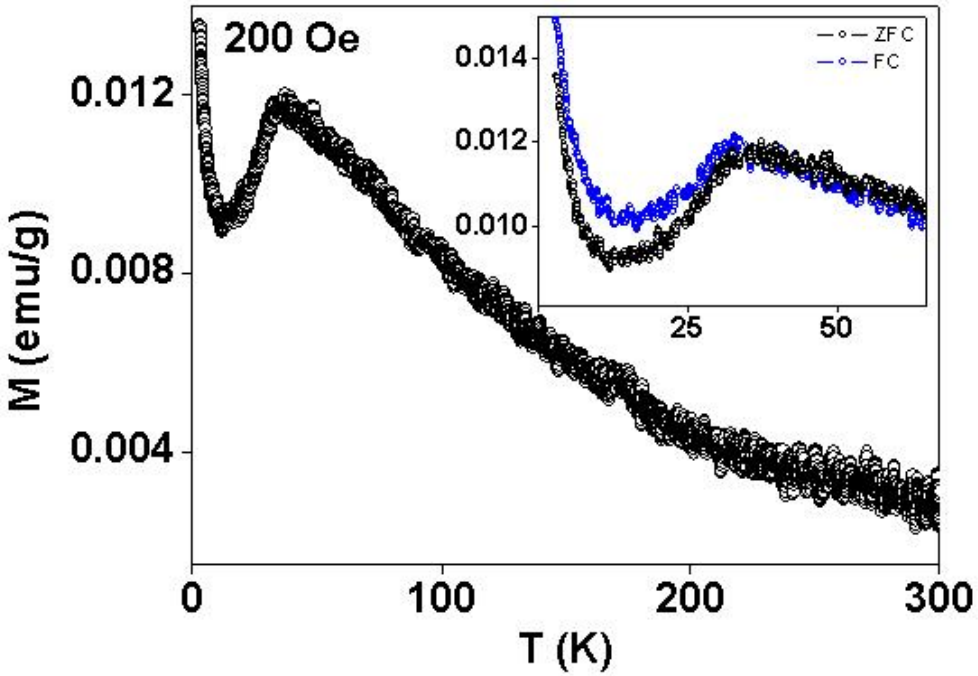

Figure S16: Magnetisation as the function of temperature. Inset shows Zero field cooled and field cooled curve of Co_3O_4 nanoparticles prepared by thermolysis of **(Co-H*F*MOF-D)** in air at 200 Oe external field.

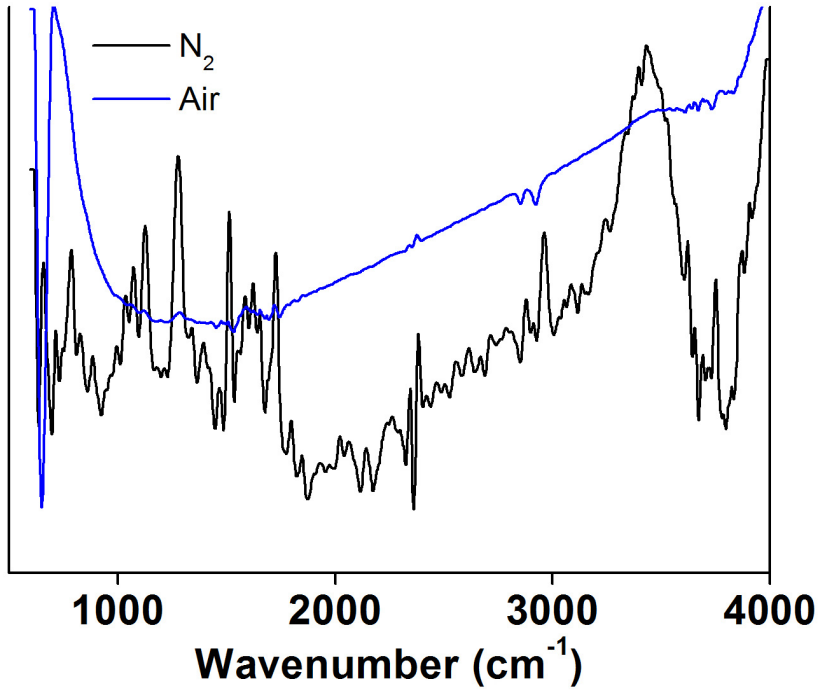

Figure S17: FTIR spectra of Co and Co_3O_4 nanoparticles prepared by thermolysis of **(Co-H*F*MOF-D)** in N_2 and air respectively.

Section 4. Detailed X-ray Photoelectron Spectroscopy (XPS) of Cu and Co nanoparticles

Next, we used the room temperature high resolution x-ray photoelectron spectroscopy (XPS), which is an extremely surface sensitive technique, to probe the surface of these particles for any oxide layer formation.

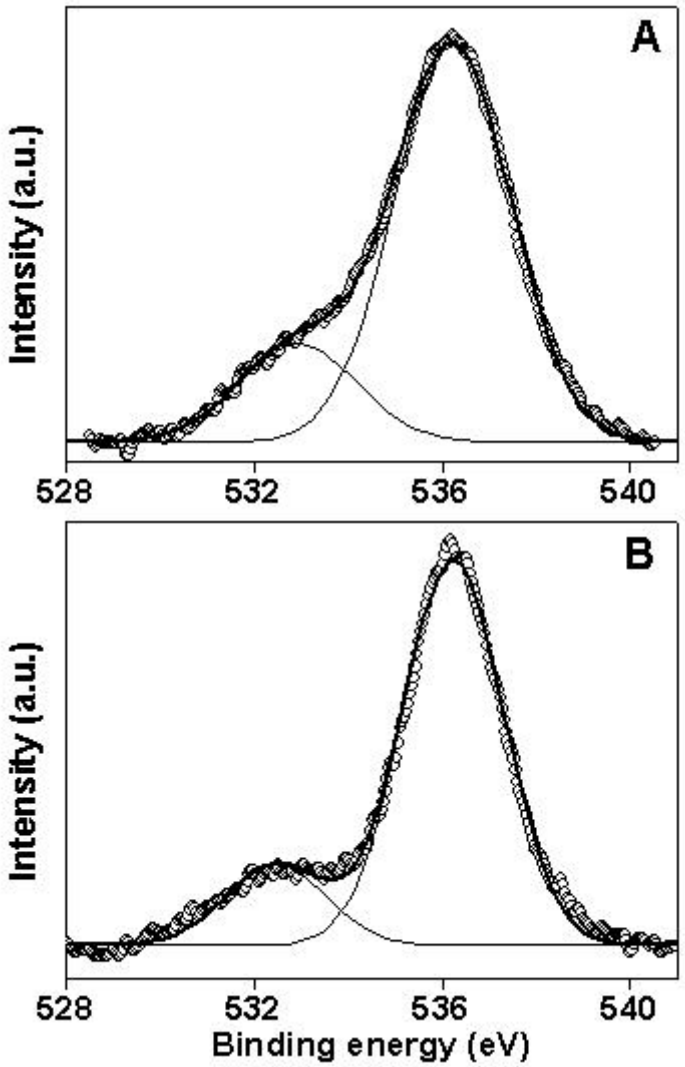

Figure S18: High resolution X-ray photoelectron spectroscopy spectra of O *1s* of (A) Cu nanoparticles (B) Co nanoparticles (scatter curves) prepared by thermolysis of **(*F*-MOF-4)** and **(Co-H*F*MOF-D).** . The lines represent the deconvoluted peaks.

Section 5. Detailed synthesis procedure, PXRD, TGA of Zn-ADA-1 and synthesis, properties of ZnO nanoparticles:

Synthesis of [Zn(ADA)(4,4'-bipy)$_{0.5}$] (Zn-ADA-1): 1.5 mL 1, 3-Adamantanediacetic Acid stock solution (0.20 M) and 0.5 mL $Zn(NO_3)_2 \cdot 6H_2O$ stock solution (0.20 M) were mixed in a 5 mL glass vial. To this solution was added 0.5 mL 4,4′-bipyridine solution (0.20 M). The vial was capped and heated to 85 ºC for 96 h. The mother liquor was decanted and the products were washed with DMF (15 mL) three times. Colorless crystals of Zn-ADA-1 were collected by filtration and dried in air (10 min) (yield: 62%, 0.0184 gm based on $Zn(NO_3)_2 \cdot 6H_2O$).

FT-IR **:** (KBr 4000-450cm^{-1}): 2897(s), 2845(w), 1618(s), 1556(w), 1423(s), 1393(w), 1223(w), 1080(w), 832(m), 755(w), 645(m), 523(m), 476(w).

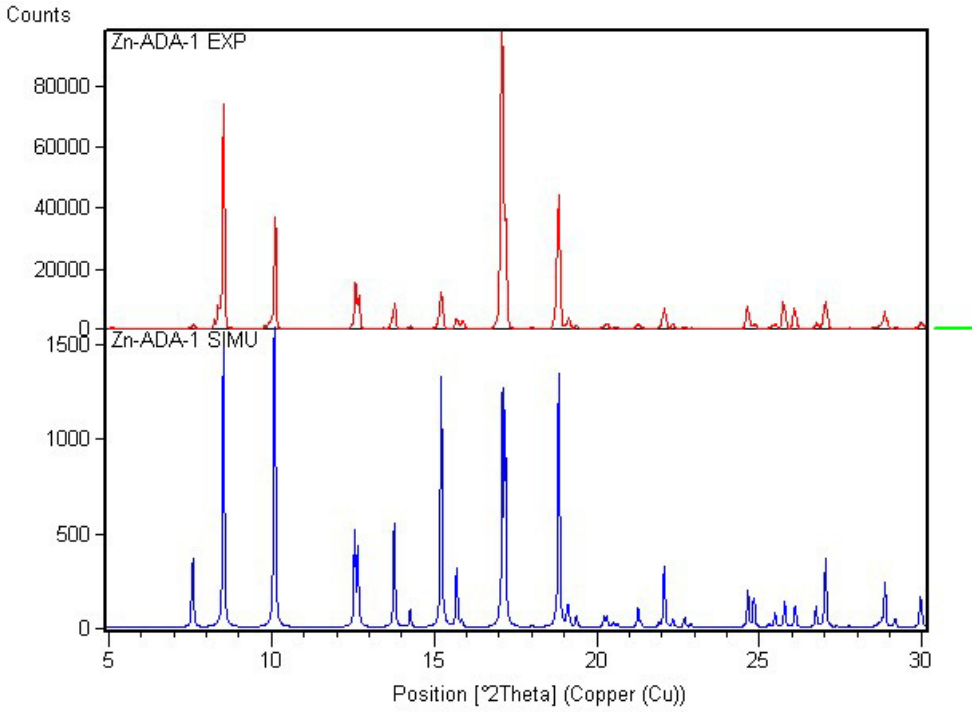

Figure S19: Comparison of the experimental PXRD pattern of as-synthesized Zn-ADA-1 (top) with the one simulated from its single crystal structure (bottom).

The as prepared [Zn(ADA)(4,4′-bipy)$_{0.5}$] **Zn-ADA-1** was taken in a silica boat and then placed in a tube furnace and heated from room temperature to 900 ◦C under N_2 with a heating rate of 10 ◦C/min to thermolyze the organic species. After reaching the target temperature, the material was cool to room temperature. The final product was black coloured powder.

The as prepared [Zn(ADA)(4,4′-bipy)$_{0.5}$] **Zn-ADA-1** was taken in a silica boat and placed in a tube furnace and heated from room temperature to 800 ◦C under air with a heating rate of 10 ◦C/min to thermolyze the organic species. After reaching, 800 ◦C the material was cool to room temperature. The final product was slightly yellowish white coloured powder.

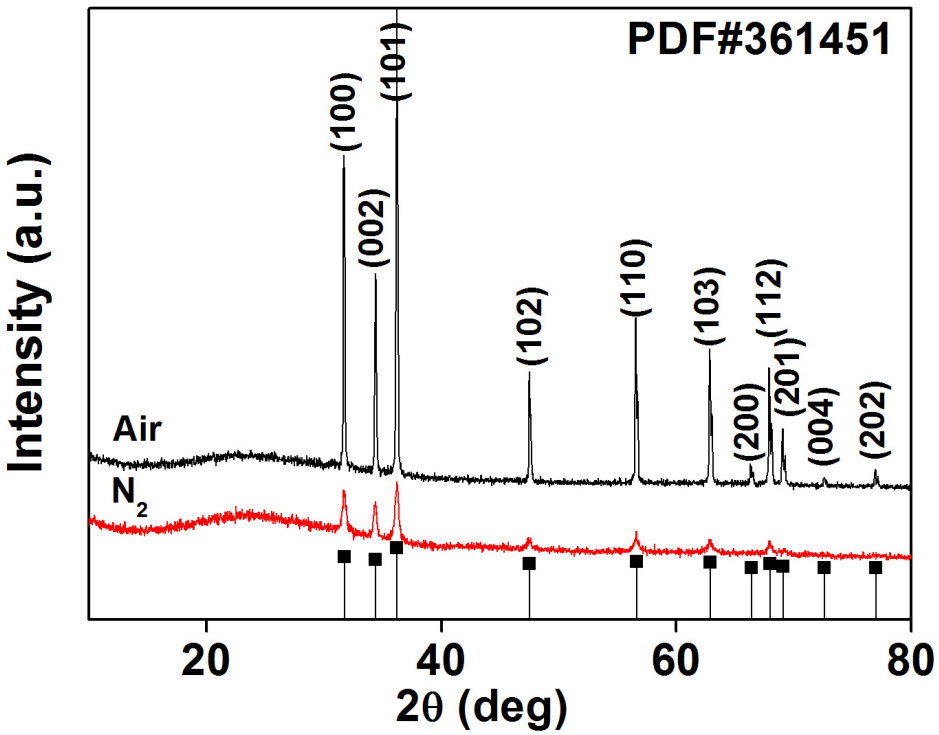

Figure S20: Powder x-ray diffraction patterns from the the JCPDS # 361451 data (black vertical line) for ZnO, ZnO nanoparticles prepared by thermolysis of (**Zn-ADA-1**) in nitrogen (black) and air (red).

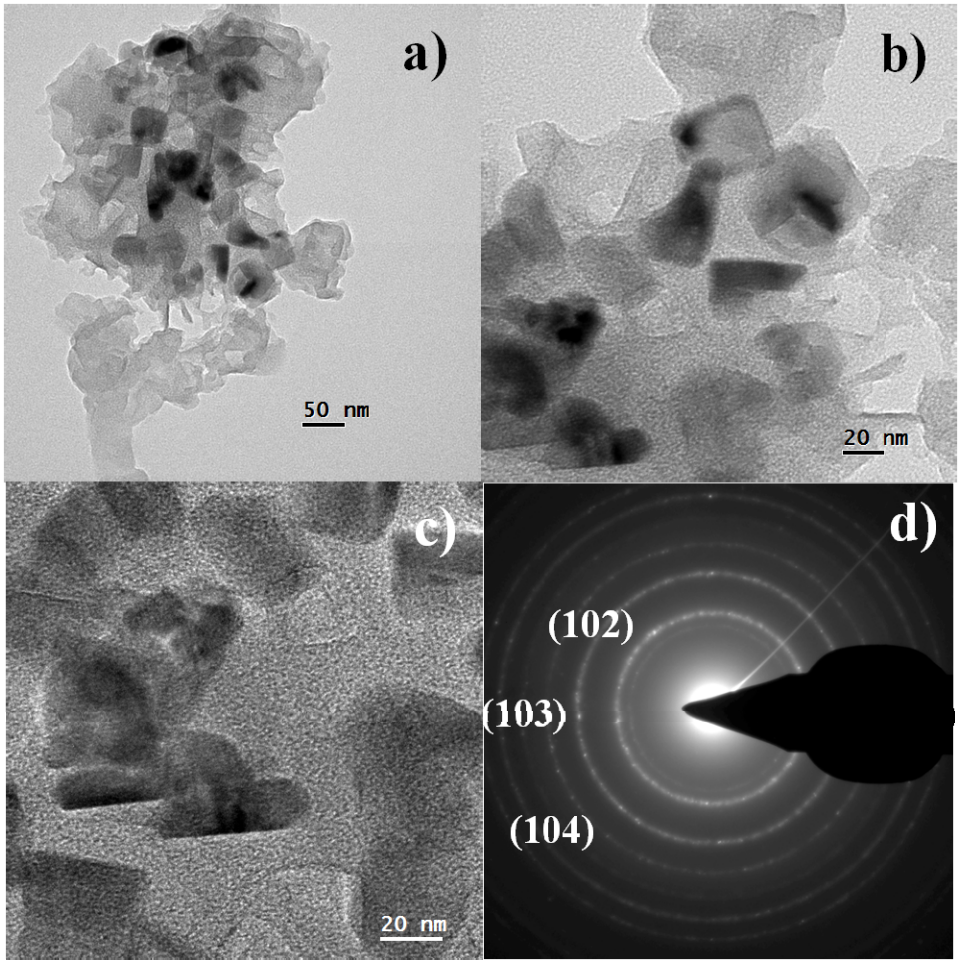

Figure S21: a-c) TEM images of ZnO nanoparticles, background shows carbon matrix b) SAED pattern of ZnO nanoparticles prepared by thermolysis of Zn-ADA-1 in nitrogen**.**

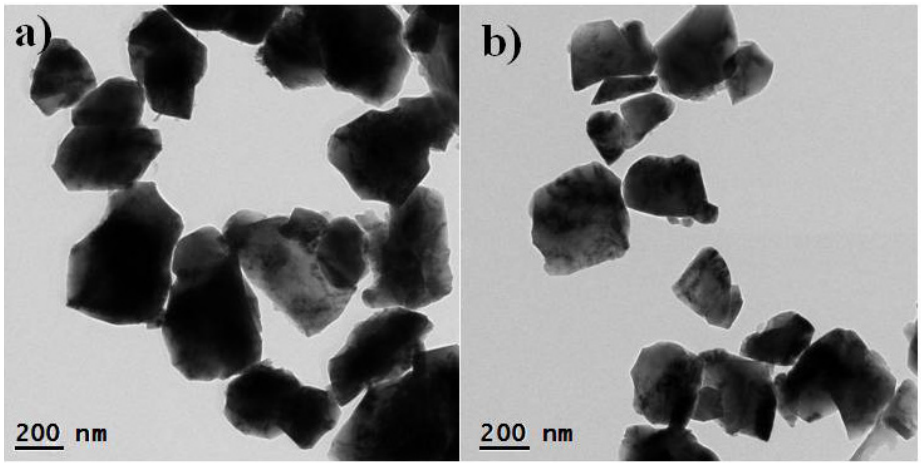

Figure S22: a,b) TEM images of ZnO nanoparticles prepared by thermolysis of **Zn-ADA-1** in air**.**

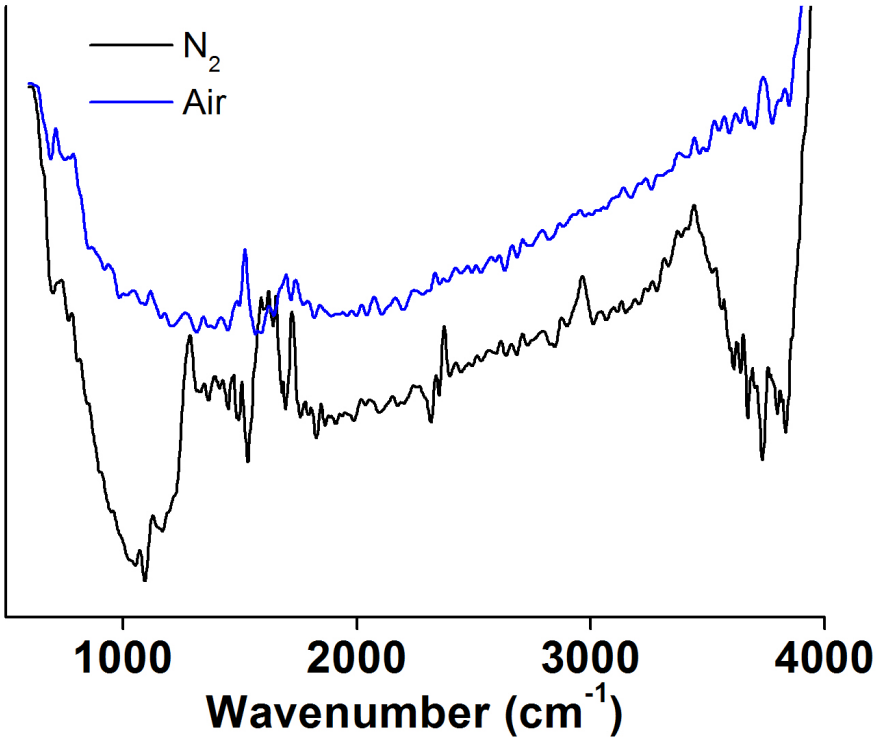

Figure S23: FTIR spectra of ZnO nanoparticles prepared by thermolysis of **(Zn-ADA-1)**.

Section 6. Detailed synthesis procedure, PXRD, TGA of α-Mg-formate and synthesis, properties of MgO nanoparticles:

Synthesis of α-Mg-formate $Mg_3(O_2CH)_6\supset[NH(CH_3)_2]_{0.5}$: As 1,3-benzene-ditetrazole is sparingly soluble in water at moderate temperature, we used the solvent DMF in which it is readily soluble. We used the solvothermal condition (Teflon-lined stainless steel autoclave at 125 to 150 °C) for synthesis which results in the formation of single crystals suitable for X-ray diffraction. Before solvothermal reactions, stirring of the heterogeneous solutions for a period 30 min was helpful for the high purity of the product. Solvothermal reaction of $Mg(CO_2\text{- }CH_3)_2 \bullet 4H_2O$ (0.214 g, 1 mmol) with 1,3-benzene-ditetrazole (0.214 g, 1 mmol) in a 25 mL Teflon-lined stainless steel autoclave in 5 mL of dimethylformamide (DMF) and 0.2 mL of HNO_3 (3.6 M) mixture at 150 °C for 60 h produces colorless crystals of $Mg_3(O_2CH)_6\supset[NH(CH_3)_2]_{0.5}$ in 61% yield. Crystals were collected by filtration and dried in air (10 min). [Yield: 61%, 0.130 g depending on $Mg(CO_2CH_3)_2\bullet 4H_2O$].

FT-IR: (KBr 4000-400 cm-1): 3302(br), 2906(w), 1683(w), 1598(s),1404(m), 1375(m), 1364(m), 841(w), 761(w), 694(w), 574(w).

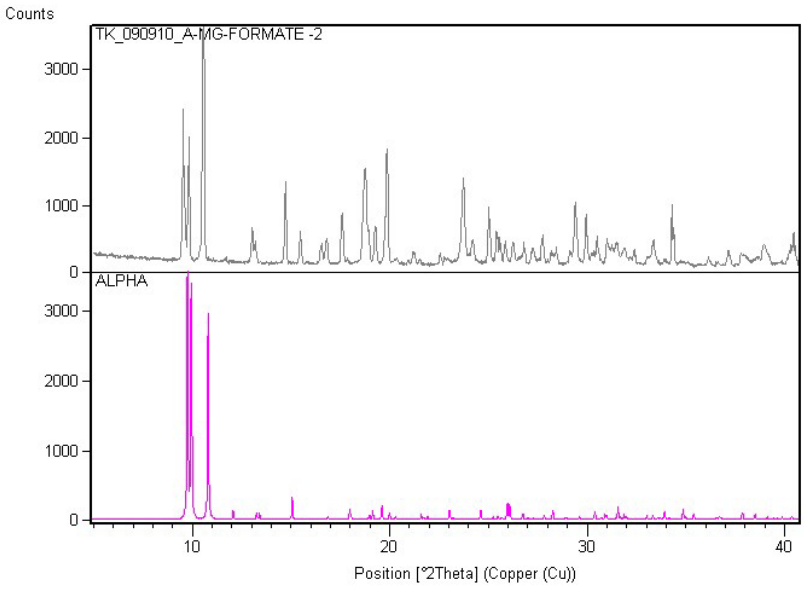

Figure S24: Comparison of the experimental PXRD pattern of as-synthesized α-MG-FORMATE (top) with the one simulated from its single crystal structure (bottom).

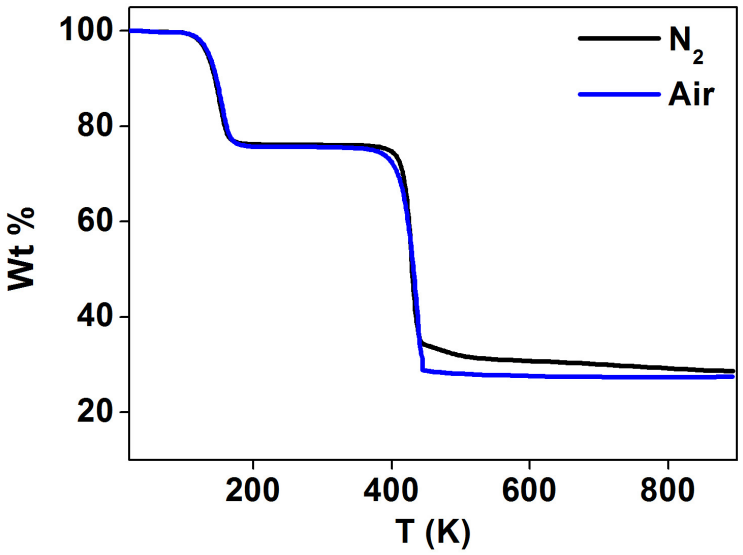

Figure S25: Thermal stability and the thermal gravimetric analysis (TGA) data of α-Mg formate.

The as prepared $[Mg_3(O_2CH)_6 \supset [NH(CH_3)_2]_{0.5}]$ α-**Mg-Formate** was taken in a silica boat and then placed in a tube furnace and heated from room temperature to 900 ◦C under N_2 with a heating rate of 10 ◦C/min to thermolyze the organic species. After reaching the target temperature, the material was cool to room temperature. The final product was black coloured powder.

The as prepared $[Mg_3(O2CH)_6 \supset [NH(CH_3)_2]_{0.5}]$ α-**Mg-Formate** was taken in a silica boat and placed in a tube furnace and heated from room temperature to 900 ◦C under air with a heating rate of 10 ◦C/min to thermolyze the organic species. After reaching, 900 ◦C the material was cool to room temperature. The final product was off white coloured powder.

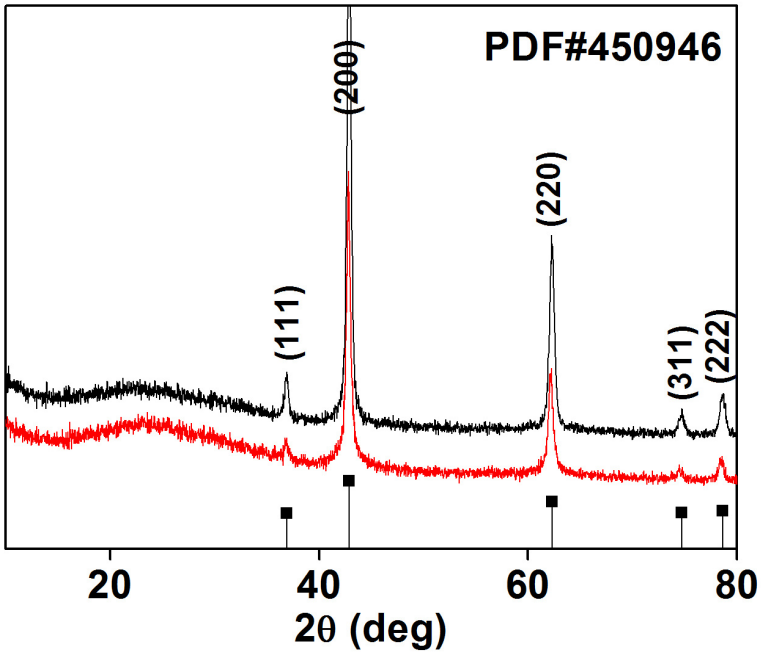

Figure S26: Powder x-ray diffraction patterns from the JCPDS # 450946 data (black vertical line) for MgO, MgO nanoparticles prepared by thermolysis of (α-**Mg-Formate**) in nitrogen (red) and air (black).

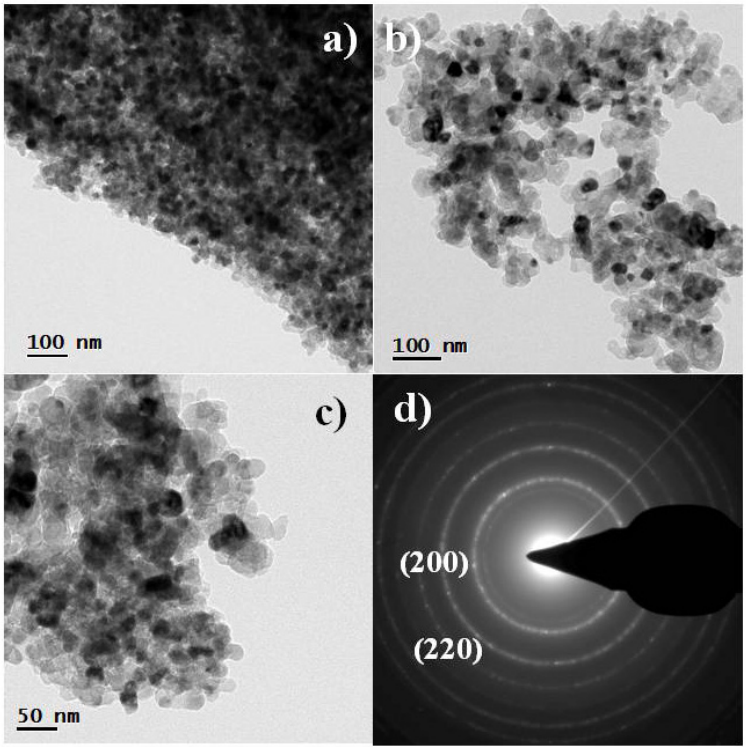

Figure S27: a-c) TEM images b) SAED pattern of MgO nanoparticles prepared by thermolysis of α-Mg-Formate in air**.**

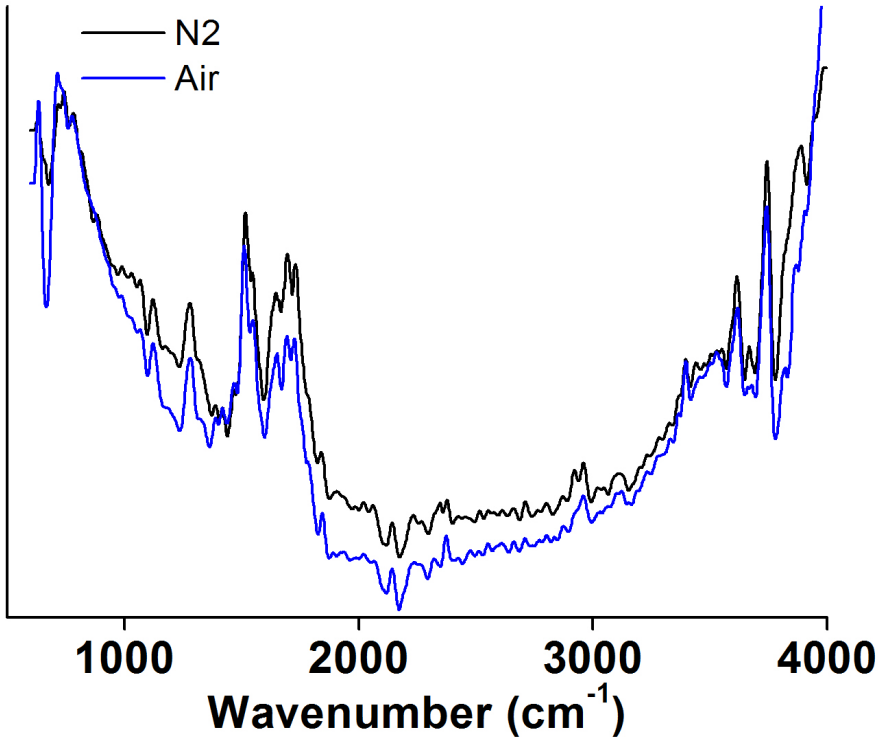

Figure S28: FTIR spectra of MgO nanoparticles prepared by thermolysis of **(**α-Mg-Formate**)**.

Section 7. Detailed synthesis procedure, PXRD, TGA of Cd-ADA-1 and synthesis, properties of CdO nanoparticles:

Synthesis of [Cd(ADA)(4,4'-bipy)$_{0.5}$]. DMF (Cd-ADA-1): 1.5 mL 1, 3-Adamantanediacetic Acid stock solution (0.20 M) and 0.5 mL $Cd(NO_3)_2 \cdot 4H_2O$ stock solution (0.20 M) were mixed in a 5 mL glass vial. To this solution was added 0.5 mL 4,4′-bipyridine solution (0.20 M). The vial was capped and heated to 85 ºC for 96 h. The mother liquor was decanted and the products were washed with DMF (15 mL) three times. Colorless crystals of Cd-ADA-1 were collected by filtration and dried in air (10 min) (yield: 58%, 0.0178 gm based on $Cd(NO_3)_2.4H_2O$).

FT-IR **:** (KBr 4000-450cm^{-1}): 3387(br, s), 3056(w), 2897(s), 2844(m), 1680(m), 1578(s), 1489(w), 1413(s), 1220(m), 1070(m), 1007(m), 808(s), 714(w), 629(m), 569(w), 491(w).

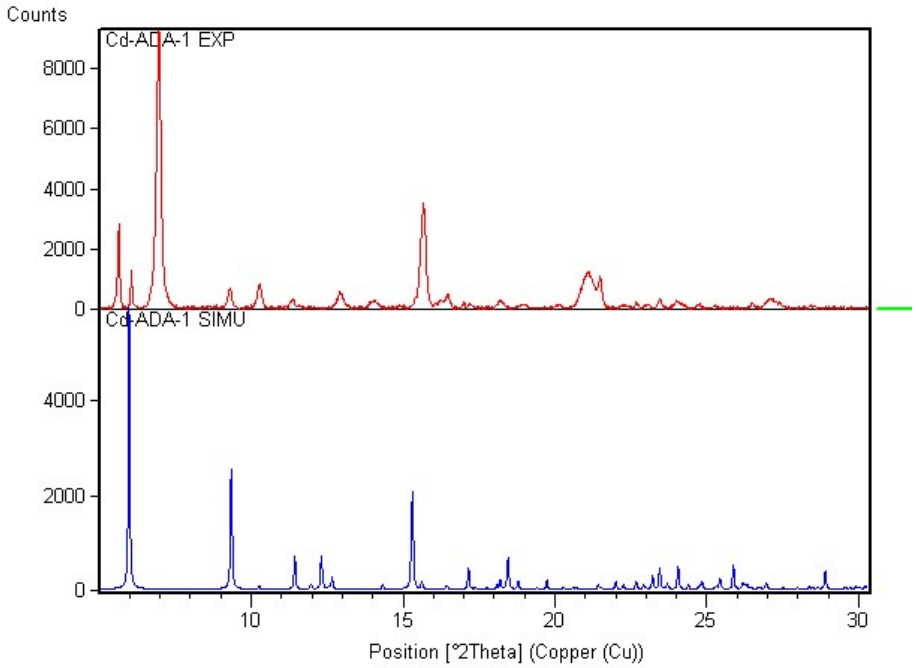

Figure S29: Comparison of the experimental PXRD pattern of as-synthesized Cd-ADA-1 (top) with the one simulated from its single crystal structure (bottom).

The as prepared [Cd(ADA)(4,4′-bipy)$_{0.5}$]• (DMF)] **Cd-ADA-1** was taken in a silica boat and then placed in a tube furnace and heated from room temperature to 900 ◦C under N_2 with a heating rate of 10 ◦C/min to thermolyze the organic species. After reaching the target temperature, the material was cool to room temperature. The final product was black coloured powder.

The as prepared [Cd(ADA)(4,4′-bipy)$_{0.5}$]• (DMF)] **Cd-ADA-1** was taken in a silica boat and placed in a tube furnace and heated from room temperature to 900 ◦C under air with a heating rate of 10 ◦C/min to thermolyze the organic species. After reaching, 900 ◦C the material was cool to room temperature. The final product was off white coloured powder.

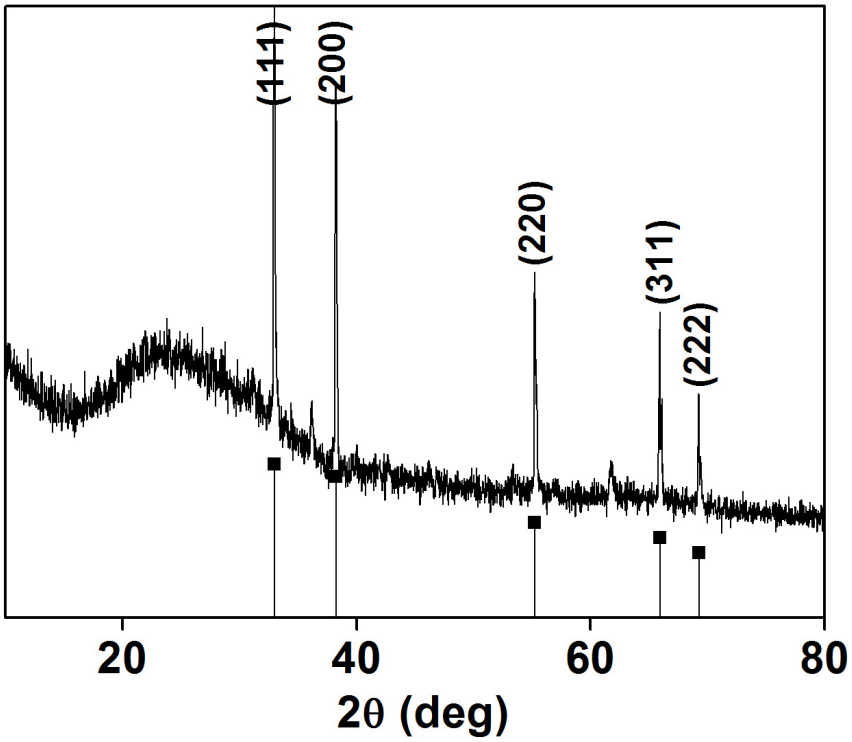

Figure S30: Powder x-ray diffraction patterns from the the JCPDS # 050640 data (black vertical line) for CdO, CdO nanoparticles prepared by thermolysis of (**Cd-ADA-1**) in air.

Section 8. Detailed synthesis procedure, PXRD, TGA of Mn-H*F*MOF-D and synthesis, properties of Mn_2O_3 nanoparticles:

Synthesis of [Mn_2(hfbba)$_2$(3-mepy)]•($H_2$0) (Mn-H*F*MOF-D) : 0.5 mL 3-methyl pyridine stock solution and 1.5 mL H_2hfbba stock solution (0.20 M) were mixed in a 5 mL vial. To this solution was added 0.5 mL $Mn(NO_3)_2$ •xH_2O stock solution (0.20 M). The vial was capped and heated to 85 °C for 96 h. The mother liquor was decanted and the products were washed with DMF (15 mL) three times. Colorless crystals of Mn-H*F*MOF-D were collected by filtration and dried in air (10 min) (Yield: 47%, 0.0134 gm depending on $Mn(NO_3)_2$ •xH_2O).

FT-IR: **(KBr 4000-450cm-1):** 3225(m, br), 1965(m), 1624(m), 1550(s), 1390(s), 1242(s), 1171(m), 957(s), 784(s), 555 (w) cm-1.

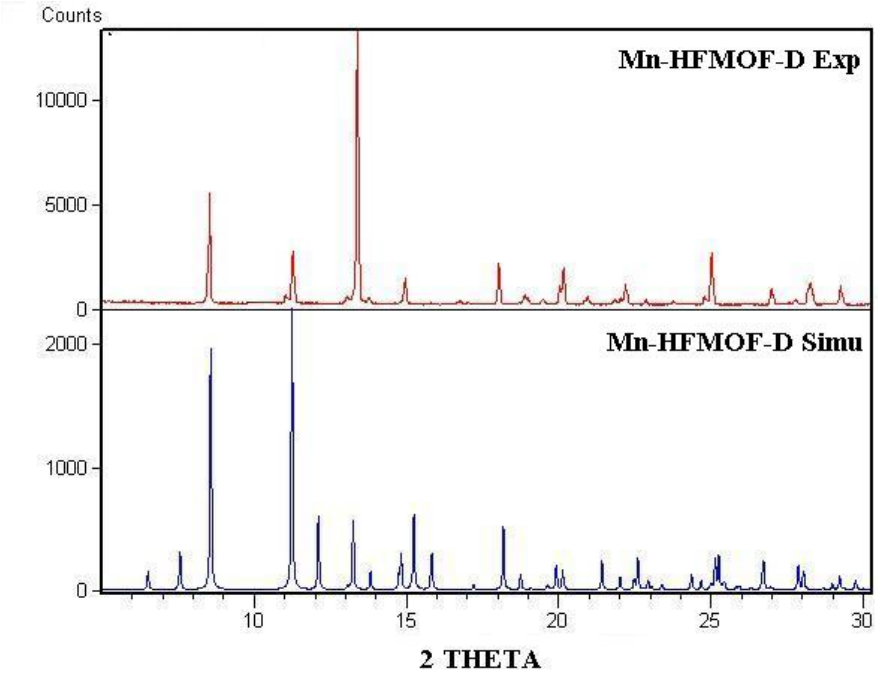

Figure S31: Comparison of the experimental PXRD pattern of as-synthesized Mn-H*F*MOF-D (top) with the one simulated from its single crystal structure (bottom).

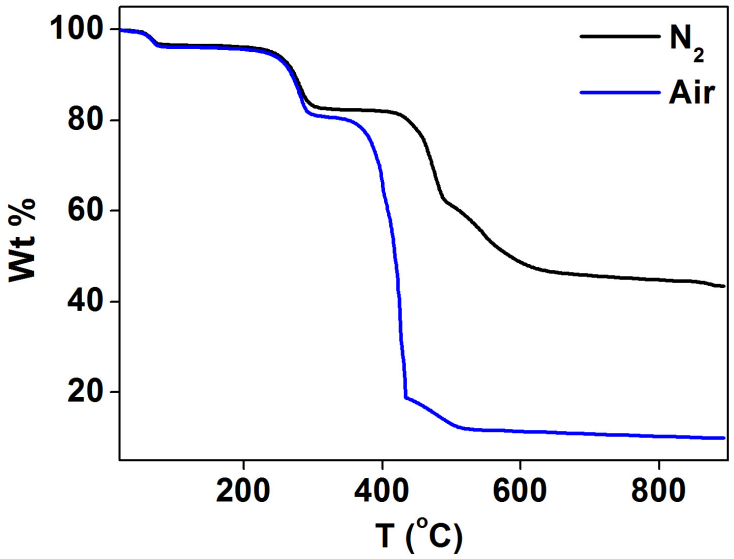

Figure S32: Thermal stability and the thermal gravimetric analysis (TGA) data of Mn-HFMOF-D in air and N_2 environment.

The as prepared [Mn_2(hfbba)$_2$(3-mepy)].(H_2O)] **Mn-H*F*MOF-D** was taken in a silica boat and then placed in a tube furnace and heated from room temperature to 900 ◦C under N_2 with a heating rate of 10 ◦C/min to thermolyze the organic species. After reaching the target temperature, the material was cool to room temperature. The final product was black coloured powder.

The as prepared [Mn_2(hfbba)$_2$(3-mepy)].(H_2O)] **Mn-H*F*MOF-D** was taken in a silica boat and placed in a tube furnace and heated from room temperature to 900 ◦C under air with a heating rate of 10 ◦C/min to thermolyze the organic species. After reaching, 900 ◦C the material was cool to room temperature. The final product was black coloured powder.

TEM images shows the Mn_2O_3 particles are of plate like morphology and has broad size distribution with average size ~150 nm embedded in carbon matrix (Figure S34). SAED image shows nice dot pattern clearly exhibiting highly crystalline nature of Mn_2O_3 nanocrystals (Figure S34b).

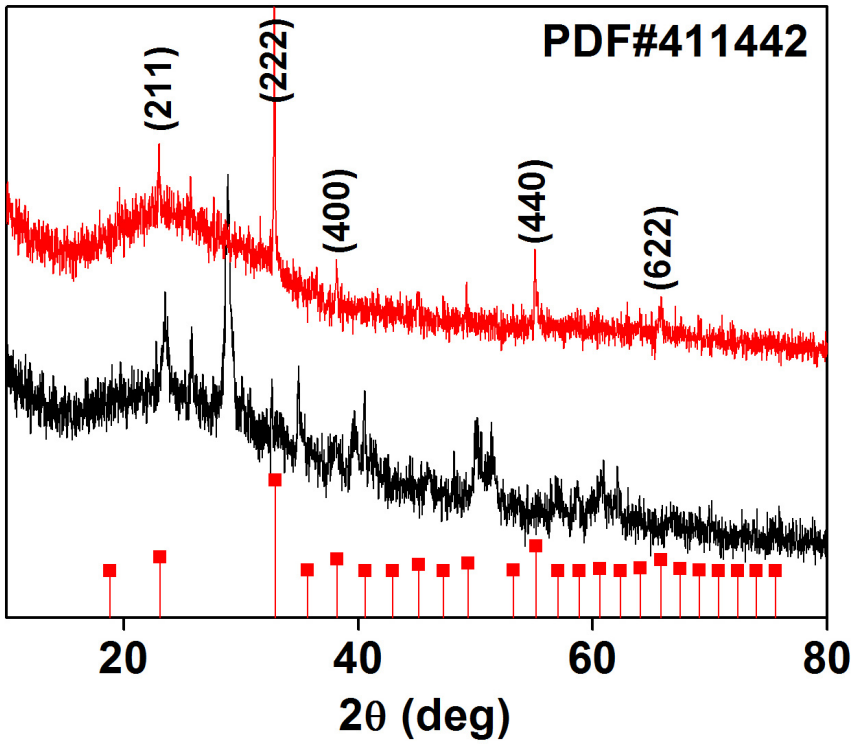

Figure S33: Powder x-ray diffraction patterns from the A) the JCPDS # 411442 data (red vertical line) for Mn_2O_3, Mn_2O_3 nanoparticles prepared by thermolysis of (**Mn-HFMOF-D**). in air (red line), unidentified phase (black line).

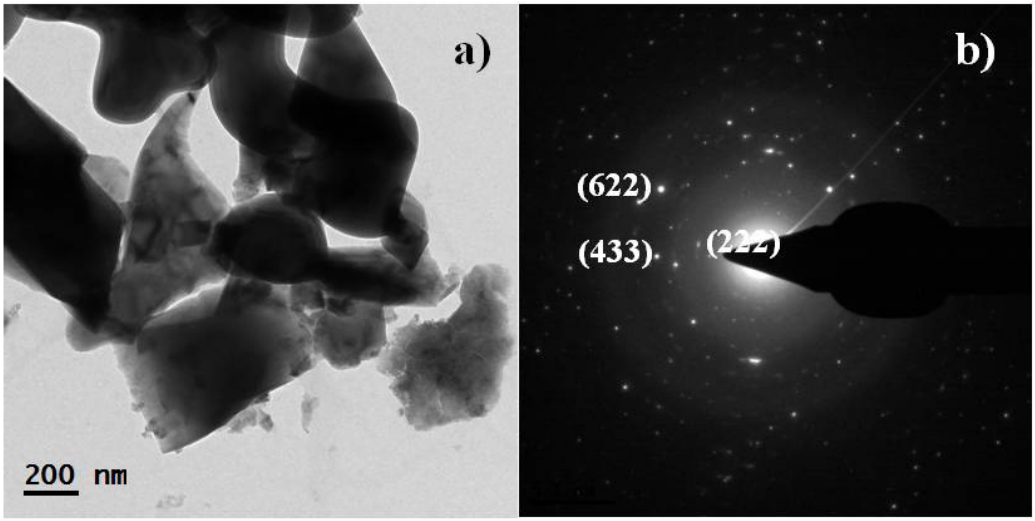

Figure S34: a) TEM images b) SAED pattern of Mn_2O_3 nanoparticles prepared by thermolysis of **Mn-HFMOF-D** in air**.**

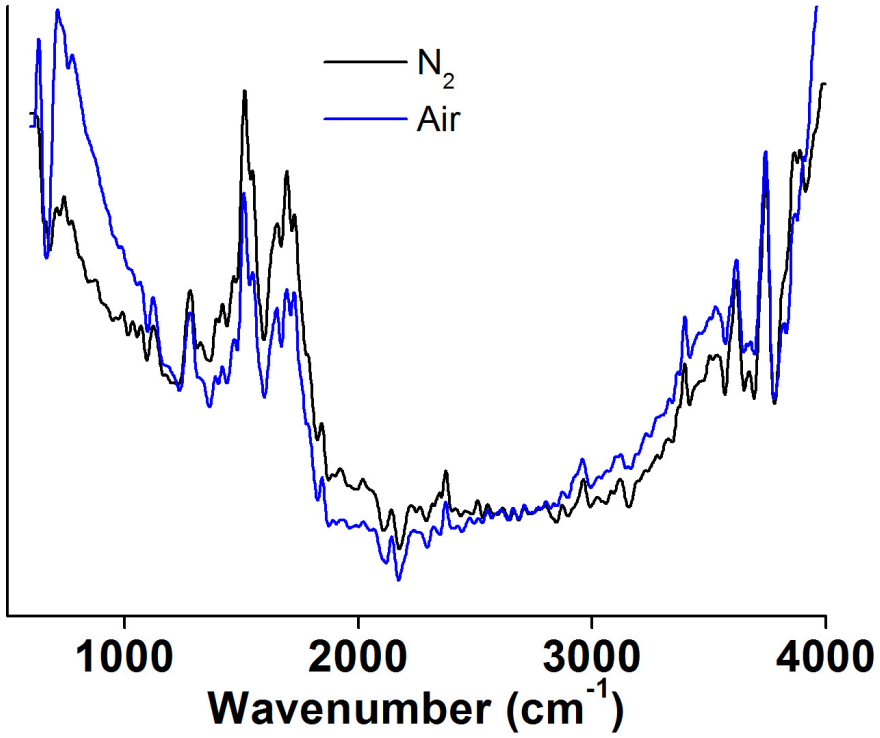

Figure S35: FTIR spectra of unknown phase and Mn_2O_3 nanoparticles prepared by thermolysis of **(Mn-HFMOF-D)** in N_2 and air respectively.

Section 9. Detailed synthesis procedure, PXRD, TGA of Cd-MOF-1 and synthesis, properties of CdS/CdO nanoparticles:

The as prepared [Cd(tdc)(bpy)(H_2O)]n **Cd-MOF-1,** MOF containing Cd and S was taken in a silica boat and then placed in a tube furnace andheated from room temperature to 900 ◦C under N_2 with a heating rate of 10 ◦C/min to thermolyze the organic species. After reaching the target temperature, the material was cool to room temperature. The final product was brownish black coloured powder.

The as prepared [Cd(tdc)(bpy)(H_2O)]n **Cd-MOF-1** was taken in a silica boat and placed in a tube furnace and heated from room temperature to 900 ◦C under air with a heating rate of 10 ◦C/min to thermolyze the organic species. After reaching, 900 ◦C the material was cool to room temperature. The final product was a off white coloured powder.

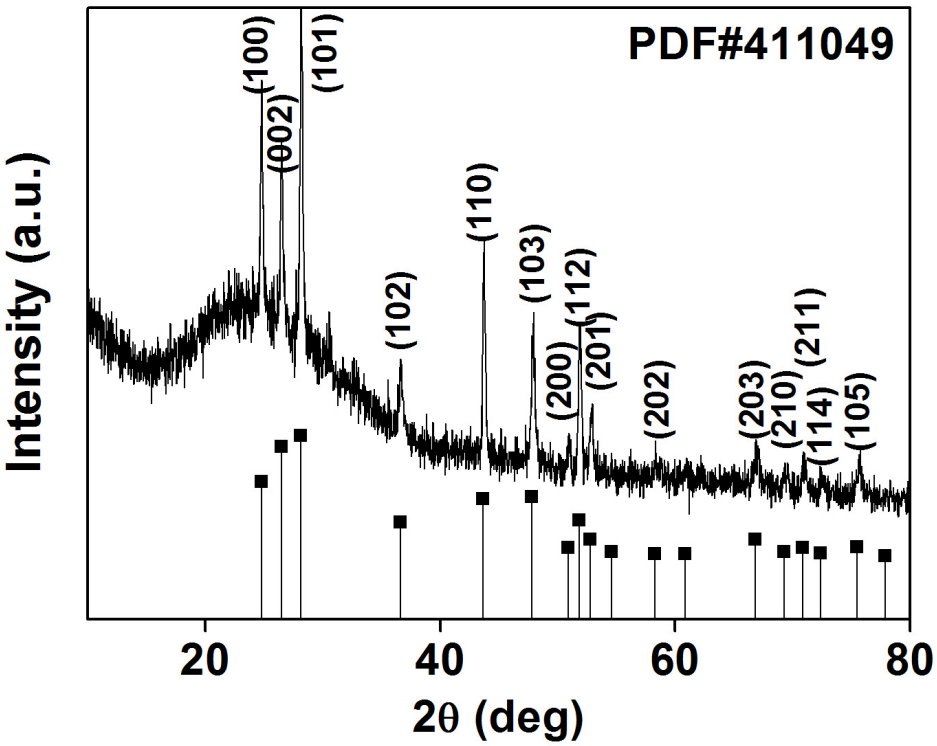

Figure S36: Powder x-ray diffraction patterns from the the JCPDS # 411049 data (black vertical line) for CdS, CdS nanoparticles prepared by thermolysis of (**Cd-MOF-1**) in nitrogen.

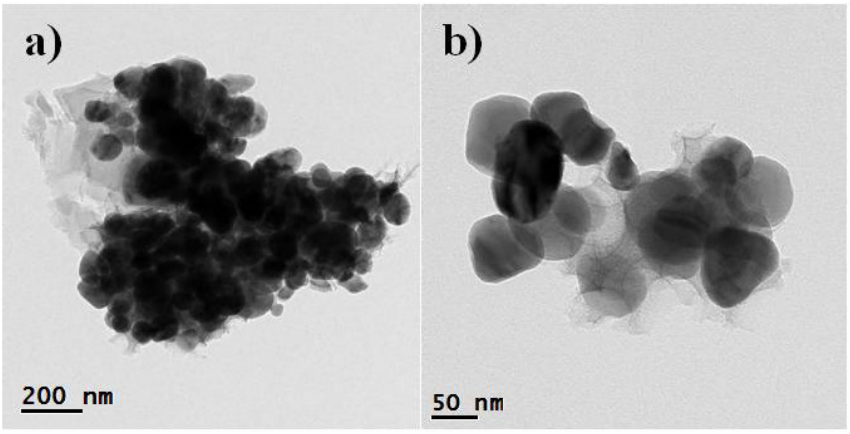

Figure S37: a,b) TEM images of CdS nanoparticles prepared by thermolysis of **Cd-MOF-1** in nitrogen**.**

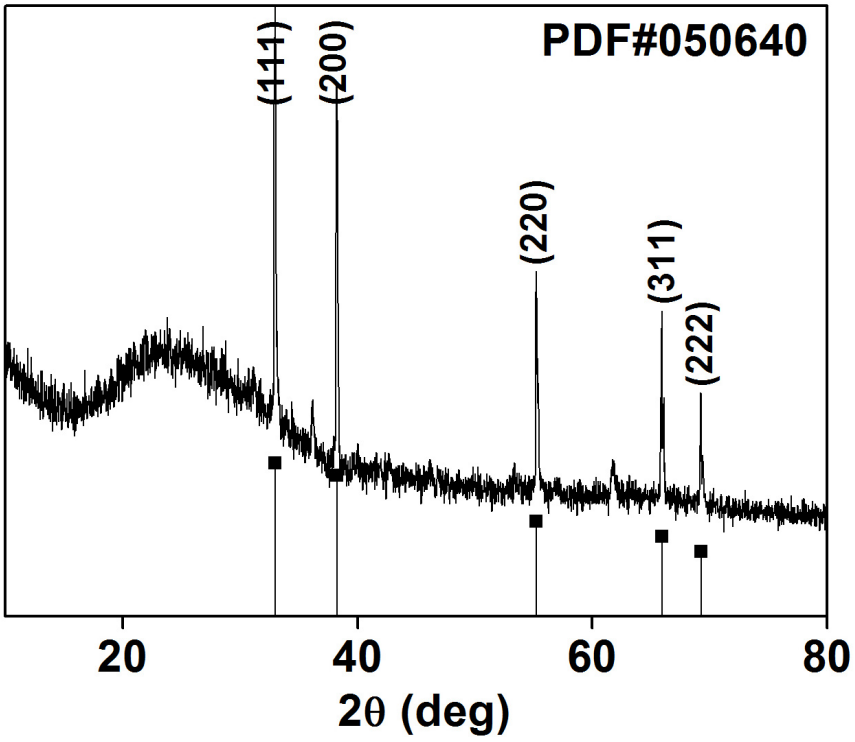

Figure S38: Powder x-ray diffraction patterns from the the JCPDS # 050640 data (black vertical line) for CdO nanoparticles prepared by thermolysis of (**Cd-MOF-1**) in air.

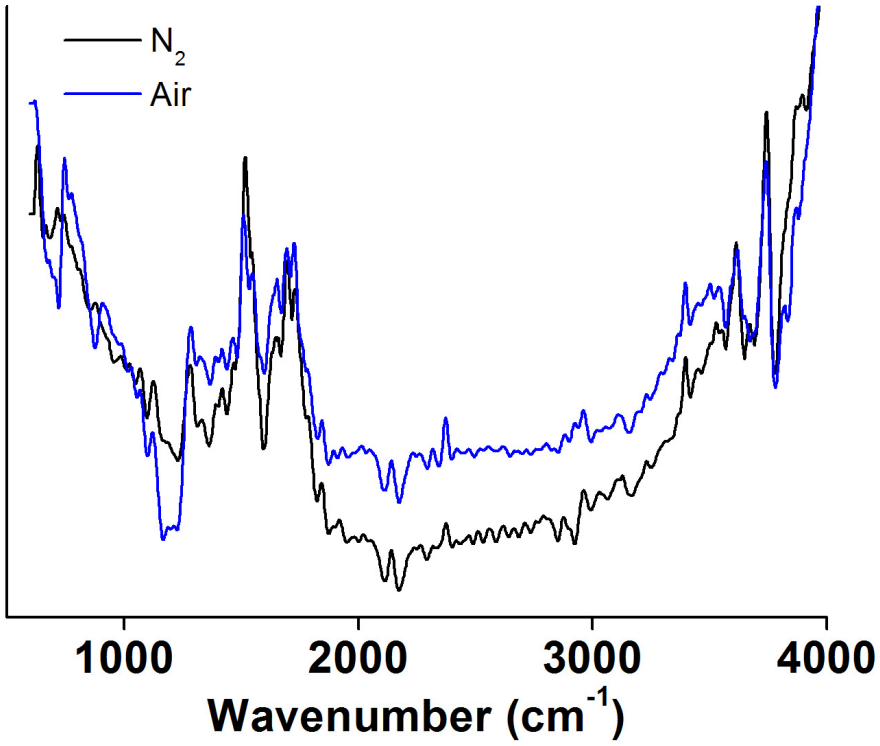

Figure S39: FTIR spectra of CdS and CdO nanoparticles prepared by thermolysis of **(Cd-MOF-1)** in N_2 and air respectively.

Section 10. Detailed synthesis procedure, PXRD, TGA of MOF-5 and synthesis, properties of ZnO nanoparticles:

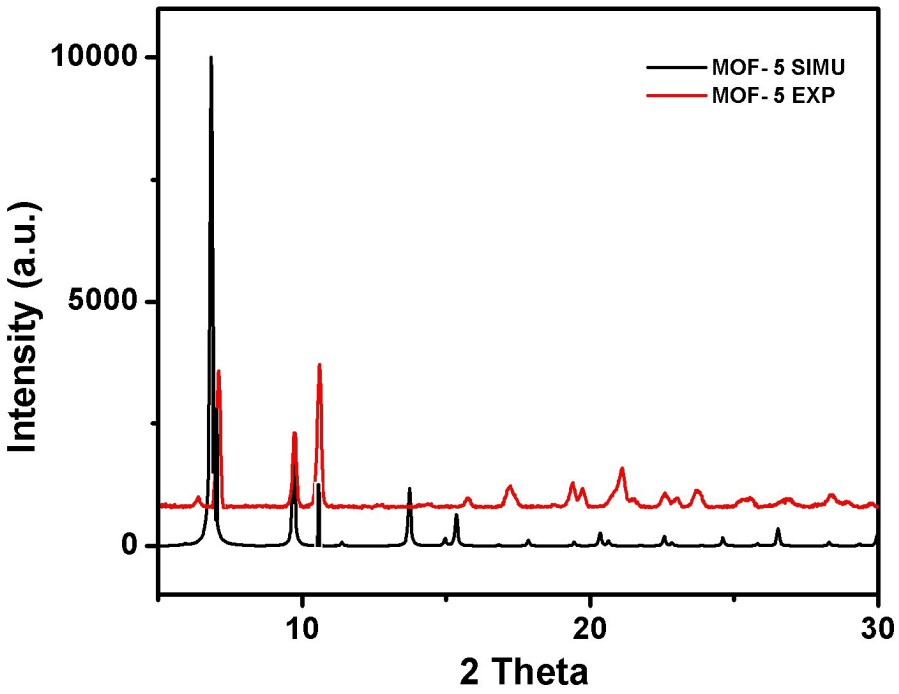

Figure S40: Comparison of the experimental PXRD pattern of as-synthesized MOF-5 (top) with the one simulated from its single crystal structure (bottom).

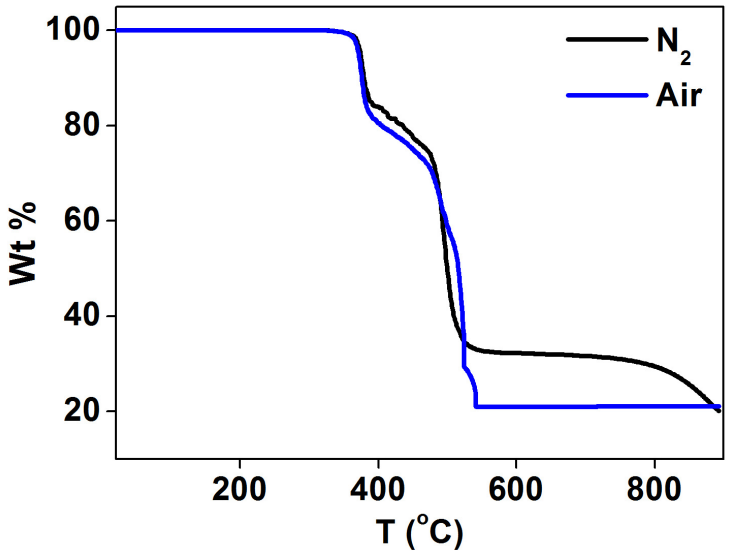

Figure S41: Thermal stability and the thermal gravimetric analysis (TGA) data of MOF-5.

The as prepared $[Zn_4O(OOCC_6H_4COO)_3]$, MOF-5 was taken in a silica boat and then placed in a tube furnace and heated from room temperature to 800 ◦C under N_2 with a heating rate of 10 ◦C/min to thermolyze the organic species. After reaching the target temperature, the material was cooled to room temperature. The final product was black coloured powder.

The as prepared $[Zn_4O(OOCC_6H_4COO)_3]$, MOF-5 was taken in a silica boat and placed in a tube furnace and heated from room temperature to 800 ◦C under air with a heating rate of 10 ◦C/min to thermolyze the organic species. After reaching, 800 ◦C the material was cooled to room temperature. The final product was black coloured powder.

The thermolysis of $[Zn_4O(OOCC_6H_4COO)_3]$, **MOF-5**[22] in nitrogen and air produces ZnO (Figure S42). The TEM images of ZnO particles (Figure S42, S44) made by thermolysis of MOF-5 in N_2 and air shows the particles are plate like in morphology and has size ~100 nm. The particles formed in both N_2 and air atmosphere are similar in size and morphology.

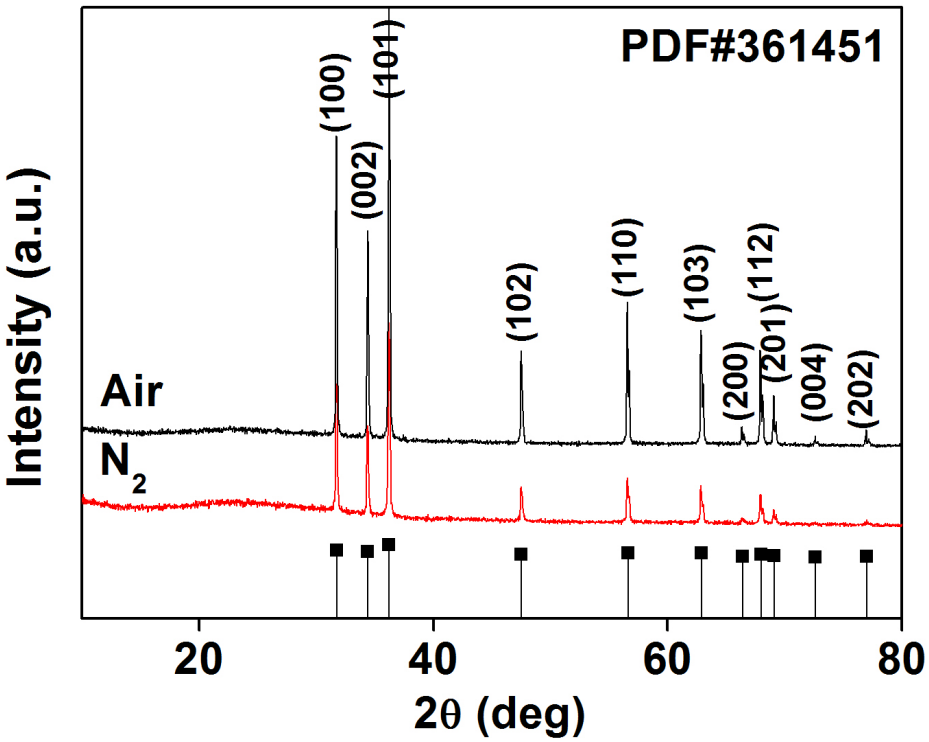

Figure S42: Powder x-ray diffraction patterns from the the JCPDS # 361451 data (black vertical line) for ZnO, ZnO nanoparticles prepared by thermolysis of (**MOF-5**) in nitrogen (red) and air (black).

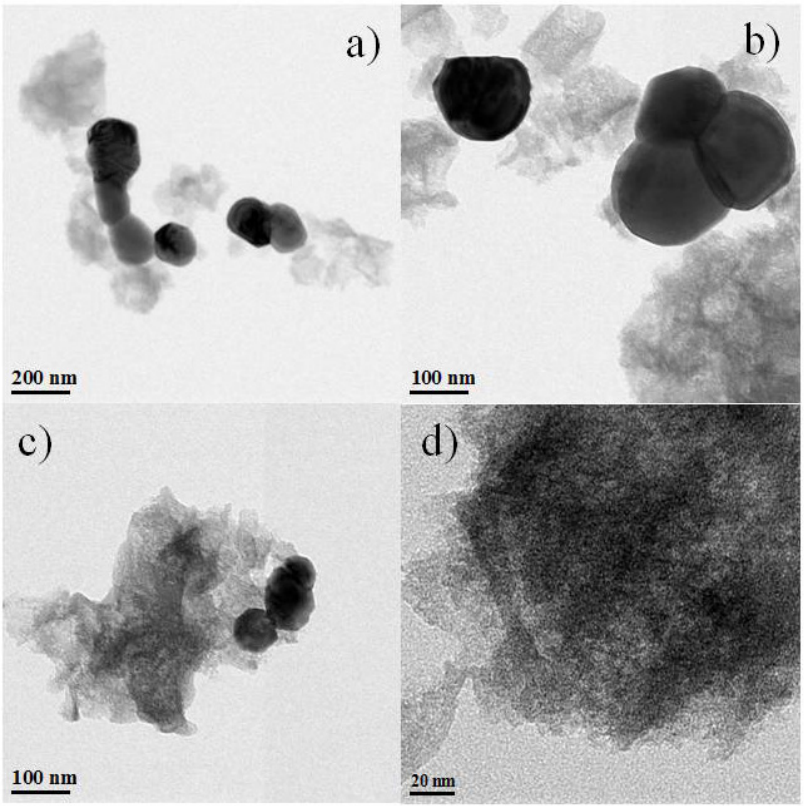

Figure S43: a,b) TEM images of ZnO nanoparticles prepared by thermolysis of MOF-5 in nitrogen**.**

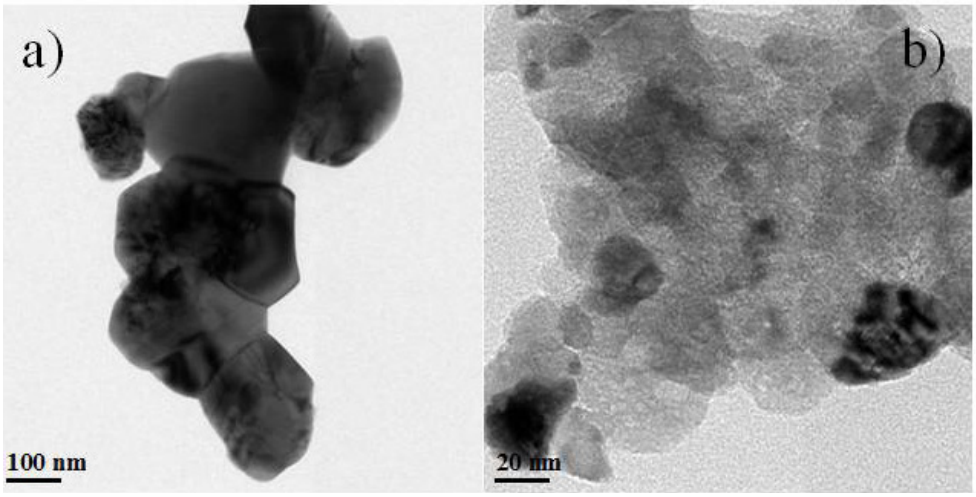

Figure S44: a,b) TEM images of ZnO nanoparticles prepared by thermolysis of MOF-5 in air**.**

Section 11. Detailed synthesis procedure, PXRD, TGA of HKUST-1 and synthesis, properties of Co/CuO particles:

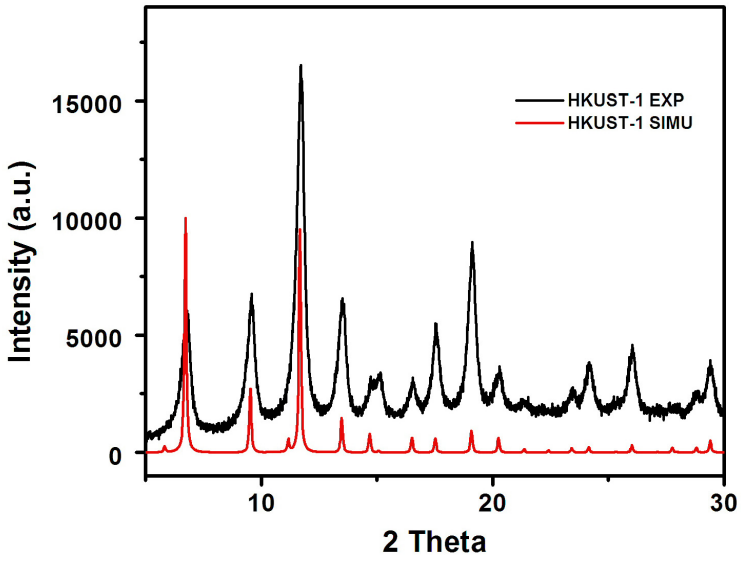

Figure S45: Comparison of the experimental PXRD pattern of as-synthesized HKUST-1 (top) with the one simulated from its single crystal structure (bottom).

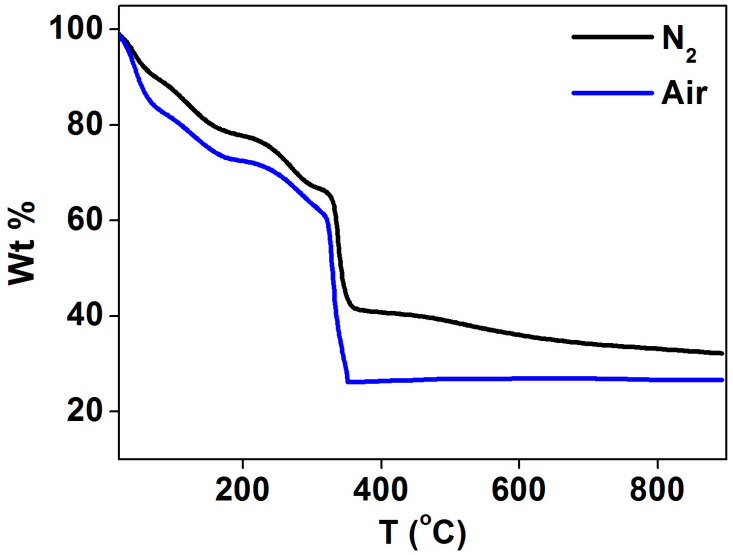

Figure S46: Thermal stability and the thermal gravimetric analysis (TGA) data of HKUST-1 in air and N_2 environment.

The as prepared $[Cu_3(TMA)_2(H_2O)_3]_n$ **HKUST-1** was taken in a silica boat and then placed in a tube furnace and heated from room temperature to 900 ◦C under N_2 with a

heating rate of 10 ◦C/min to thermolyze the organic species. After reaching the target temperature, the material was cool to room temperature. The final product was a black coloured powder.

The as prepared $[Cu_3(TMA)_2(H_2O)_3]_n$ **HKUST-1** was taken in a silica boat and placed in a tube furnace and heated from room temperature to 900 ◦C under air with a heating rate of 10 ◦C/min to thermolyze the organic species. After reaching, 900 ◦C the material was cool to room temperature. The final product was a black coloured powder.

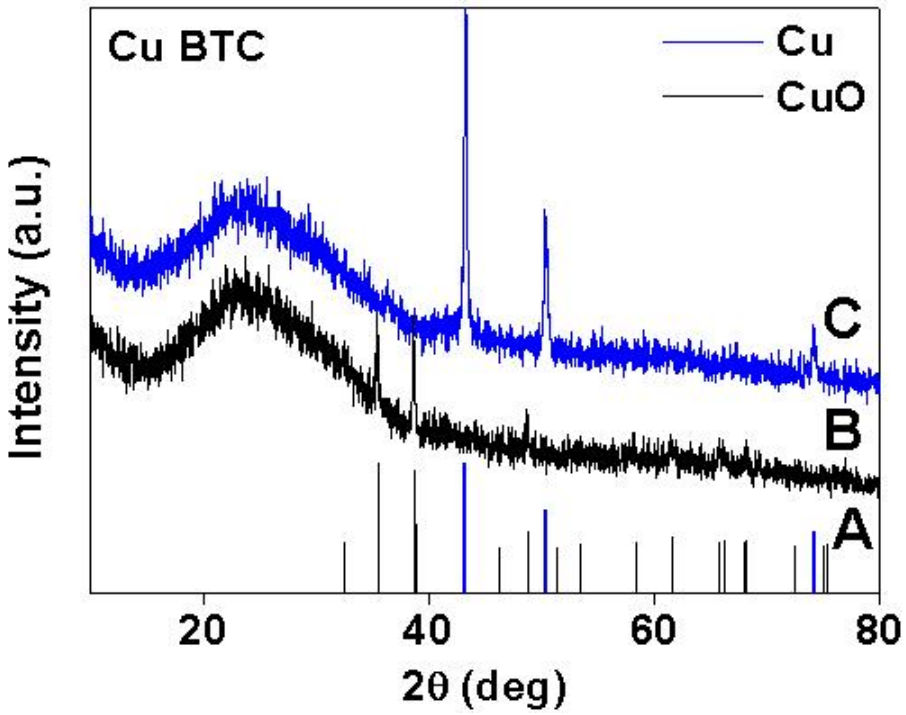

Figure S47: Powder x-ray diffraction patterns from A) the JCPDS # 031005 database for Cu (blue line) and JCPDS # 450937 (black line) database for CuO B) CuO nanoparticles and C) Cu nanoparticles prepared by thermolysis of HKUST-1.

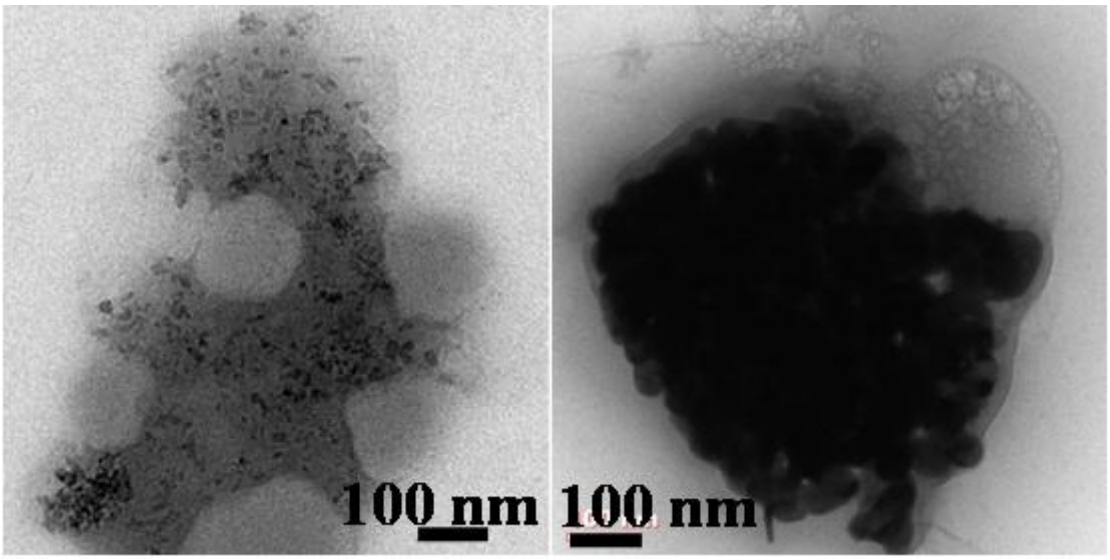

Figure S48: Transmission electron micrograph of Cu nanocrystals prepared by thermolysis of HKUST-1.

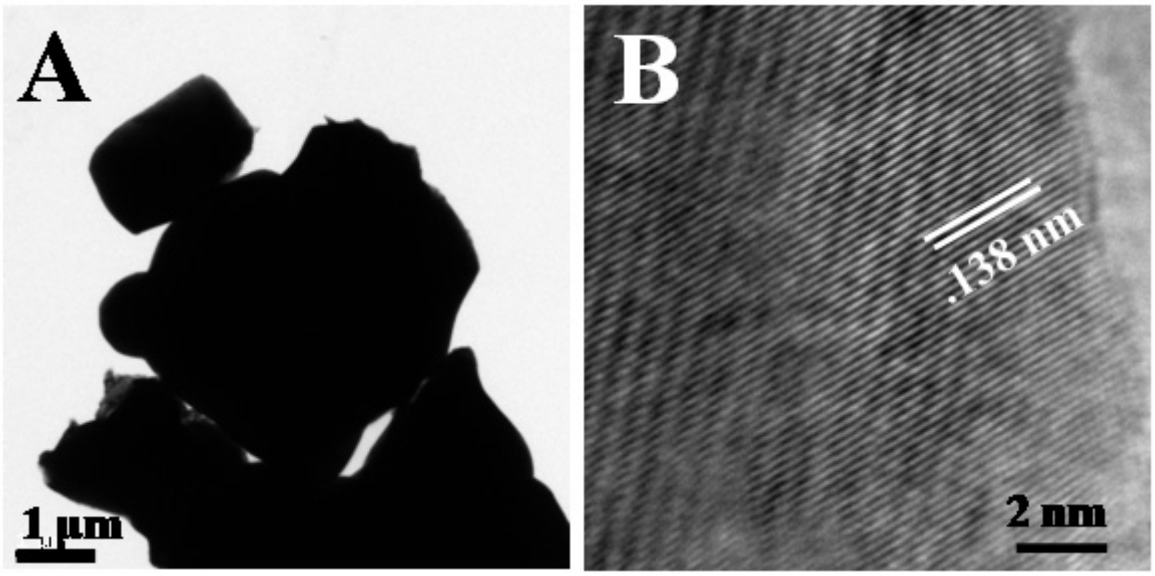

Figure S49: A) Transmission electron micrograph, B) high resolution TEM images showing the lattice fringes of CuO crystals prepared by thermolysis of HKUST-1.

Section 12. Detailed synthesis procedure, PXRD, TGA of MOF-CJ4 and synthesis, properties of Co/Co_3O_4 nanoparticles:

Synthesis of MOF-CJ4: MOF-CJ4 was synthesized from the solvothermal reaction of $Co(NO_3)_2$• 6H2O and 1,3,5 benzenetricarboxylic acid (H3BTC) in the mixed solvents of N,N-dimethylformamide (DMF) (7.5 mL) and glacial acetic acid (HAc) (2.5 mL). Typically, 1,3,5-H_3BTC (0.5 mmol, 0.105 g) and $Co(NO_3)_2 \cdot 6H_2O$ (0.5 mmol, 0.147 g) were dissolved into mixed solvents (DMF/HAc) ($Co(NO_3)_2 \cdot 6H_2O$:1 1,3,5-H_3BTC:390 DMF:176 HAc) and heated at 170 °C for 2 days. The final product containing large purple hexagonal prismatic crystals were obtained. Single crystals was washed thoroughly with DMF and dried at room temperature. Yield: 54%. Anal. Calcd. for MOF-CJ4.

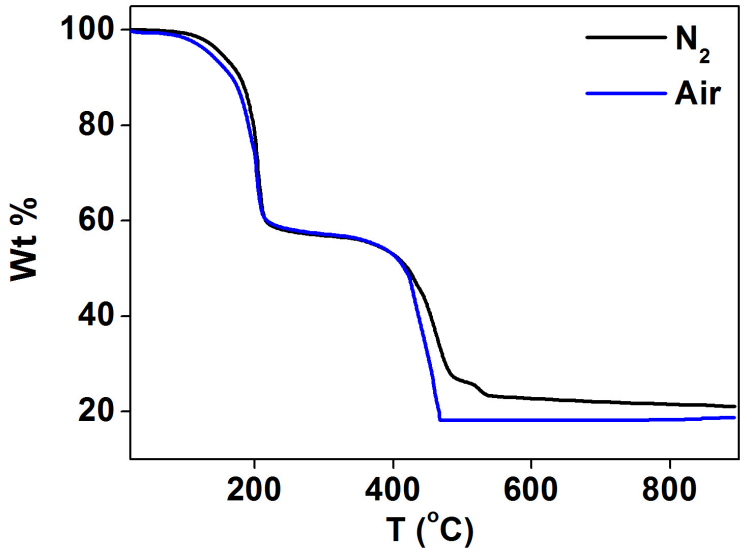

Figure S50: Thermal stability and the thermal gravimetric analysis (TGA) data of Co-BTC in air and N_2 environment.

The as prepared $[Co_6(BTC)_2(HCOO)_6(DMF)_6]$ **MOF-CJ4** was taken in a silica boat and then placed in a tube furnace and heated from room temperature to 900 ◦C under N_2 with

a heating rate of 10 ◦C/min to thermolyze the organic species. After reaching the target temperature, the material was cool to room temperature. The final product was a black coloured powder.

The as prepared $[Co_6(BTC)_2(HCOO)_6(DMF)_6]$ **MOF-CJ4** was taken in a silica boat and placed in a tube furnace and heated from room temperature to 900 ◦C under air with a heating rate of 10 ◦C/min to thermolyze the organic species. After reaching, 900 ◦C the material was cool to room temperature. The final product was a black coloured powder.

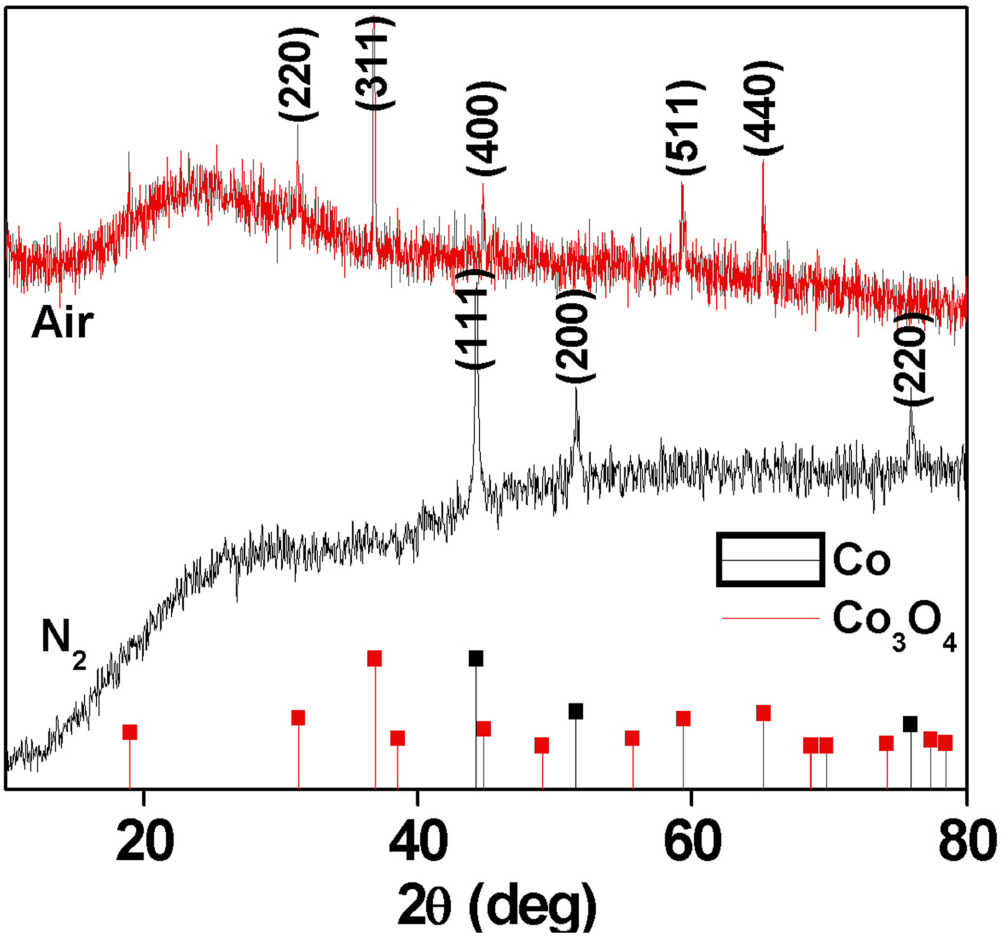

Figure S51: Powder x-ray diffraction patterns from the A) the JCPDS # 150806 data (black line) for Co and JCPDS # 431003(red lines) data for Co_3O_4. B) Co_3O_4 and C) Co nanoparticles prepared by thermolysis of (**MOF-CJ4**) in air and N_2 respectively.

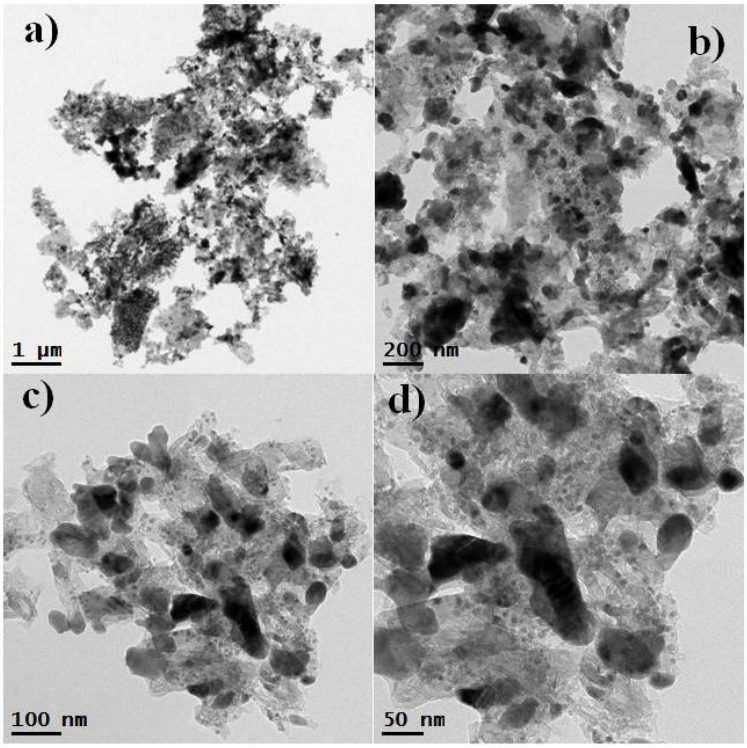

Figure S52: a-d) TEM images of Co nanoparticles prepared by thermolysis of Co-BTC in nitrogen**.**

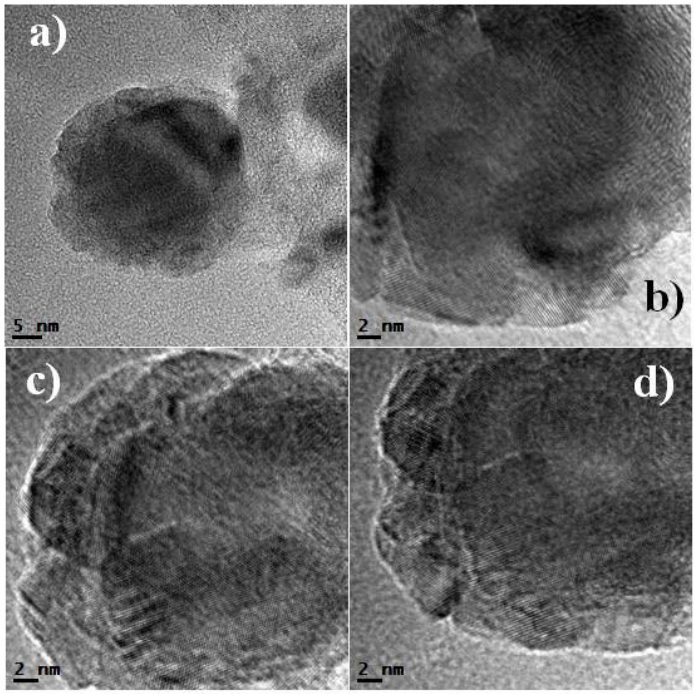

Figure S53: a-d) HR-TEM images of Co nanoparticles prepared by thermolysis of Co-BTC in nitrogen**.** These images show that particles are formed by aggregation of small crystallite to form the bigger particles during the reaction.

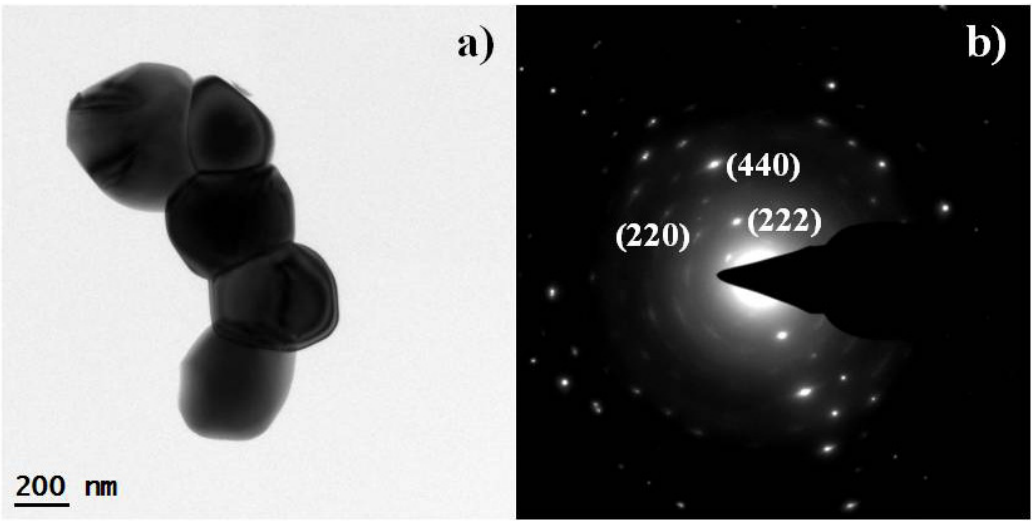

Figure S54: a) TEM images b) SAED pattern of Co_3O_4 nanoparticles prepared by thermolysis of Co-BTC in air**.**

Section 13. Detailed synthesis procedure, PXRD, TGA of Cu-TBA-2, -2F and synthesis, properties of Cu/CuO nanoparticles:

Cu_2(4-TBA)$_2$(DMF)(C_2H_5OH) (Cu-TBA-2): 2.0 mL 4-TBA solution (0.20 M) in 1:1 solution of DMF and EtOH was taken in a 5 mL vial. 0.009 gm (0.2 mmol) of anhydrous CuCl solid was added to this solution. Additional 0.5 ml of DMF was added to this above mixture followed by vial was capped and heated at 90 °C for 72 h. After cooling to room temperature, two layers were seen, one is a plate light blue crystal of Cu-TBA-2 and other one is an unreacted white starting materials. Then collected Cu-TBA-2 crystals were washed with EtOH (2 ml X 3) and DMF (5 ml X 2) and dried in air (10 min). [**Yield:** 61 %, 0.0054 gm depending on CuCl].

FT-IR: (KBr 4000-600 cm^{-1}): 3555(m, br), 2811(m), 2675(w), 2361(w), 1668(s), 1614(m), 1537(w), 1401(s), 1325(m), 1098(s), 860(m), 739(s) cm^{-1}.

Cu_2(2-F-4-TBA)$_2$(DMF)$_2$ (Cu-TBA-2F): 2.0 mL 2-F-4-TBA solution (0.20 M) in 1:1 solution of DMF and EtOH was taken in a 5 mL vial. 0.5 mL $Cu(NO_3)_2$. $3H_2O$ solution (0.20 M) in DMF was added to this solution. The vial was capped and heated to 85 °C for 96 h. The mother liquor was decanted and plate blue crystals were filtered off, washed with EtOH and dried in air (10 min). [**Yield:** 58 %, 0.0139 gm depending on $Cu(NO_3)_2$. $3H_2O$].

FT-IR: (KBr 4000-600 cm^{-1}): 3561(m, br), 2923(m), 2853(w), 2458(w), 1745(s), 1537(s), 1380(s), 1212(s), 1090(m), 1020(s), 895(m), 752(s) cm^{-1}.

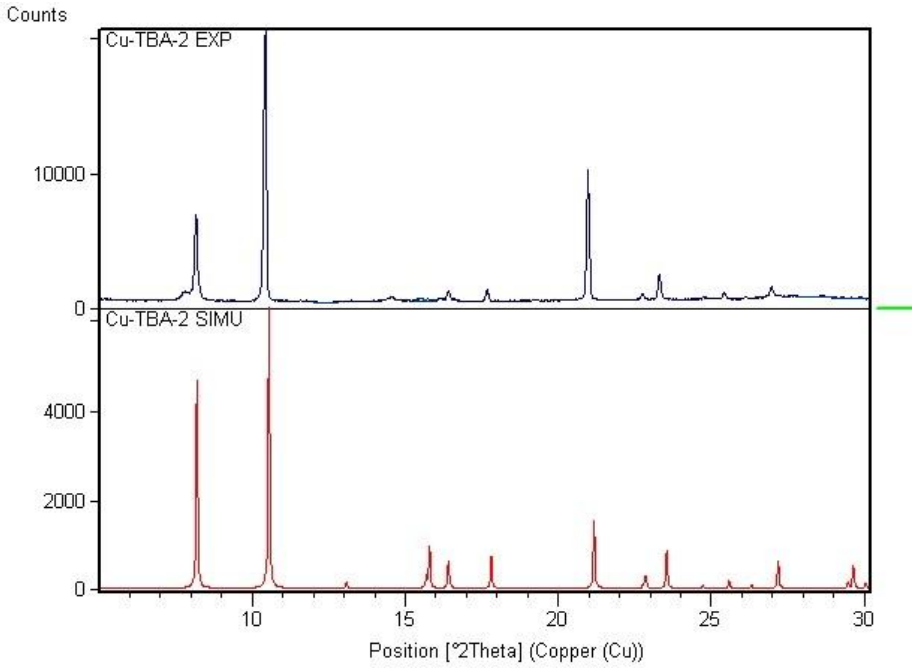

Figure S55: Comparison of the experimental PXRD pattern of as-synthesized Cu-TBA-2 (top) with the one simulated from its single crystal structure (bottom).

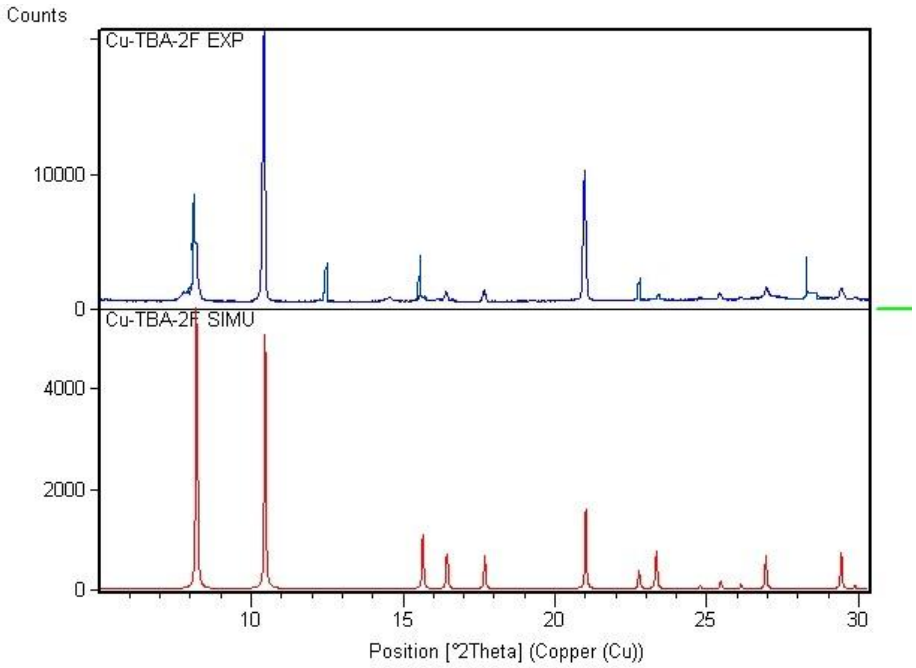

Figure S56: Comparison of the experimental PXRD pattern of as-synthesized Cu-TBA-2F (top) with the one simulated from its single crystal structure (bottom).

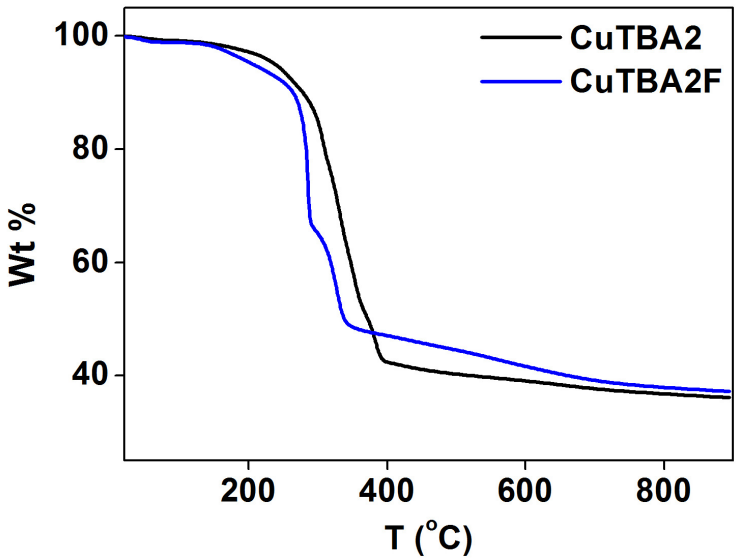

Figure S57: Thermal stability and the thermal gravimetric analysis (TGA) data of Cu-TBA-2 and Cu-TBA-2F in nitrogen.

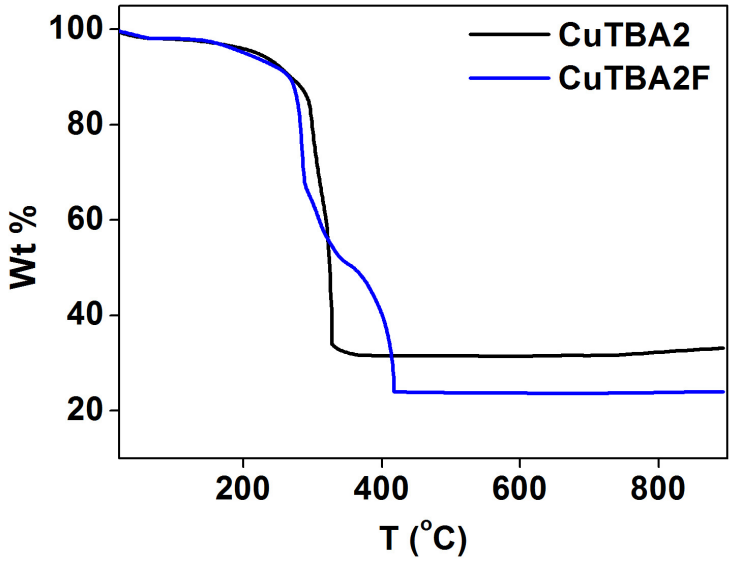

Figure S58: Thermal stability and the thermal gravimetric analysis (TGA) data of Cu-TBA-2 and Cu-TBA-2F in air.

The as prepared Cu-TBA-2 was taken in a silica boat and then placed in a tube furnace and heated from room temperature to 900 ◦C under N_2 with a heating rate of 10 ◦C/min to thermolyze the organic species. After reaching the target temperature, the material

was cool to room temperature. The final product was a black coloured powder. Similar experiment was done on CuTBA-2F, here also final product was a black coloured powder.

The as prepared Cu-TBA-2 was taken in a silica boat and placed in a tube furnace and heated from room temperature to 900 ◦C under air with a heating rate of 10 ◦C/min to thermolyze the organic species. After reaching, 900 ◦C the material was cool to room temperature. The final product was a black coloured powder. Similar experiment was done on CuTBA-2F, here also final product was a black coloured powder.

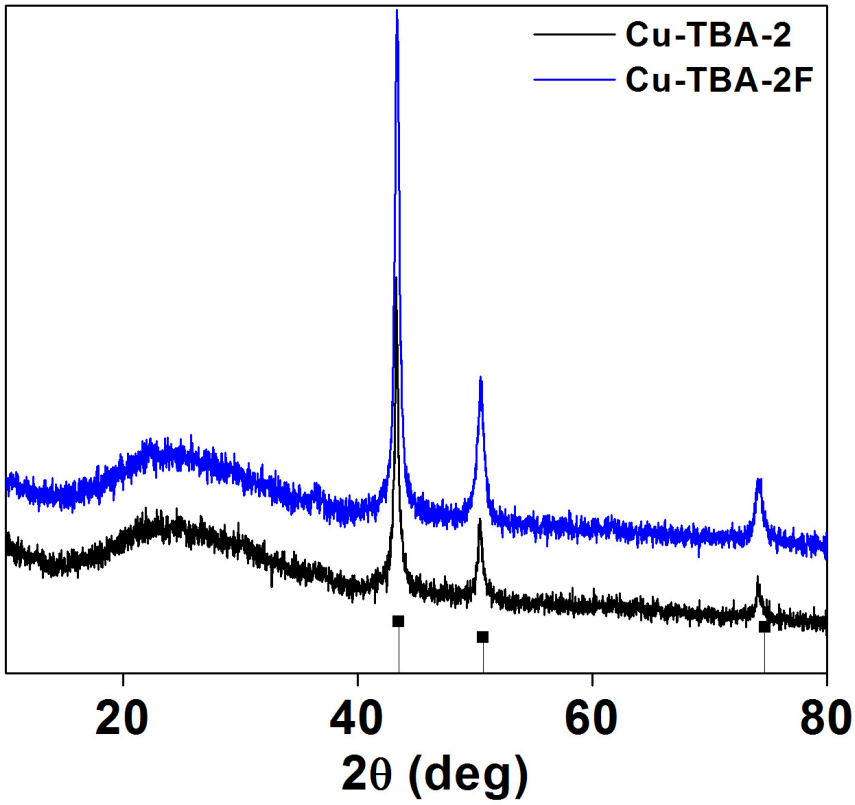

Figure S59: Powder x-ray diffraction patterns from A) the JCPDS # 031005 database for Cu (blue line)) Cu nanoparticles prepared by thermolysis of Cu-TBA 2 and Cu-TBA 2F in nitrogen.

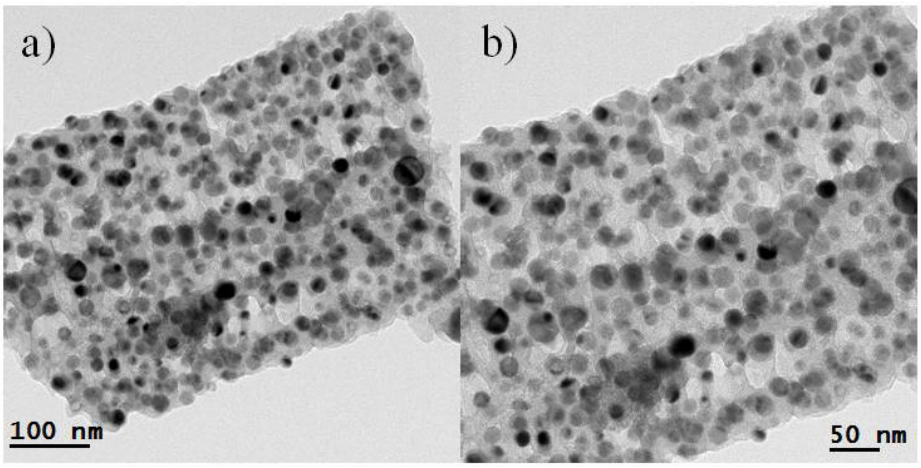

Figure S60: A,B) TEM images of Cu nanoparticles prepared by thermolysis of Cu-TBA-2 in nitrogen.

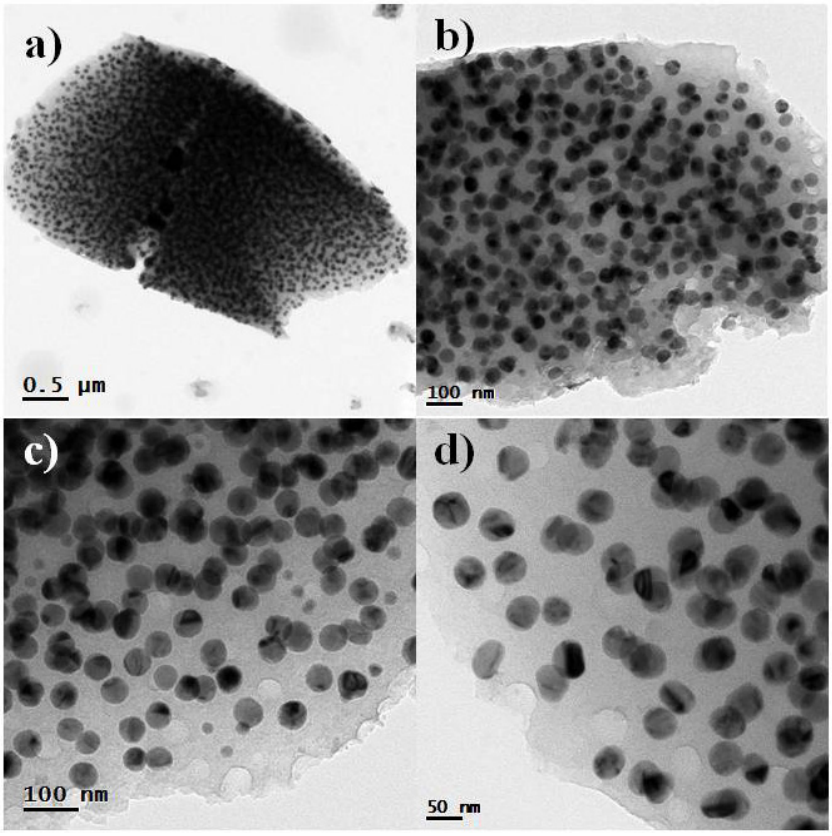

Figure S61: A,B) TEM images of Cu nanoparticles prepared by thermolysis of Cu-TBA-2F in nitrogen.

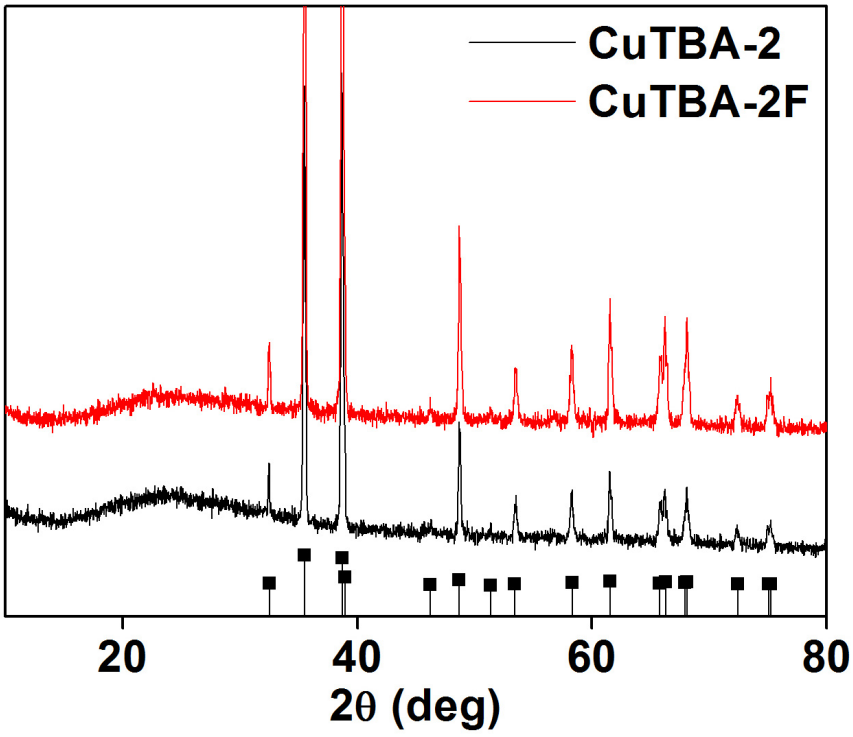

Figure S62: Powder x-ray diffraction patterns from the JCPDS # 450937 database for CuO and CuO nanoparticles prepared by thermolysis of Cu-TBA 2 and Cu-TBA 2F in air.

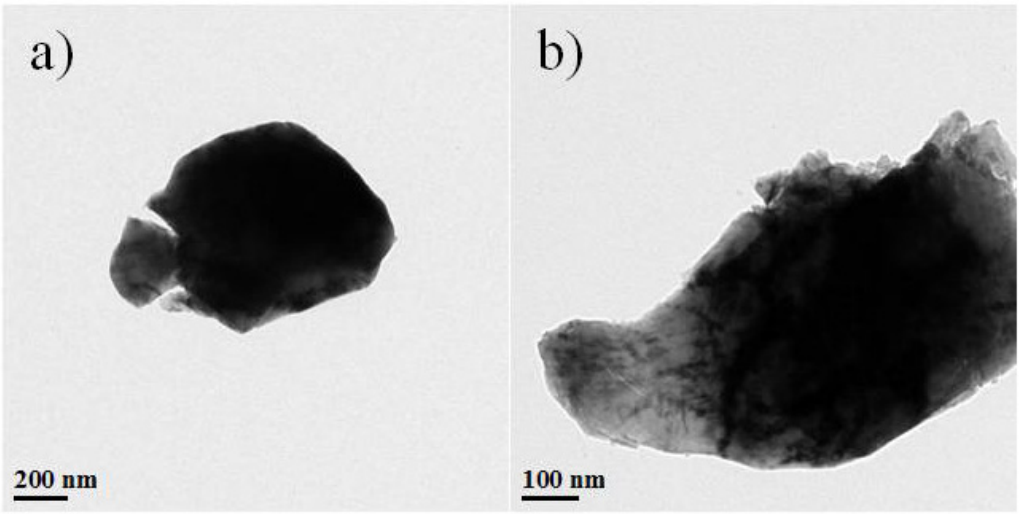

Figure S63: A,B) TEM images of CuO nanoparticles prepared by thermolysis of Cu-TBA-2 in air.

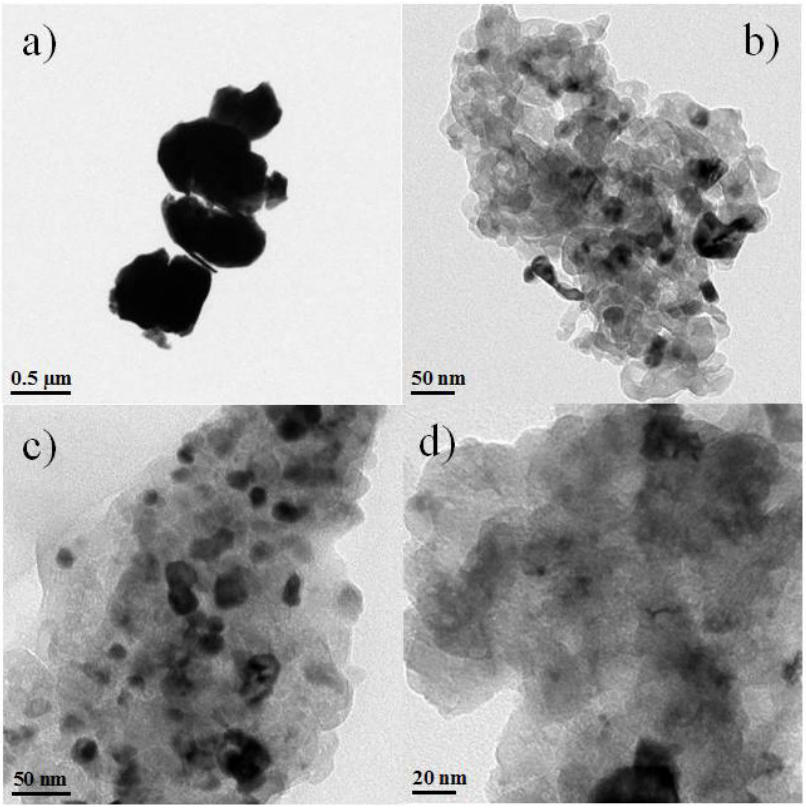

Figure S64: A,B) TEM images of CuO nanoparticles prepared by thermolysis of Cu-TBA-2F in air.

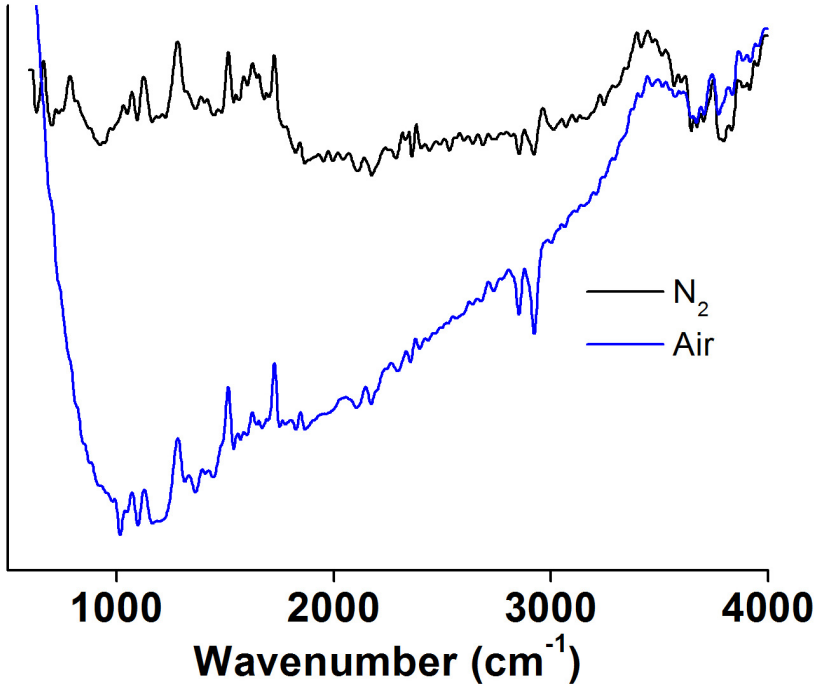

Figure S65: FTIR spectra of Cu and CuO nanoparticles prepared by thermolysis of **(Cu-TBA-2)** in N_2 and air respectively.

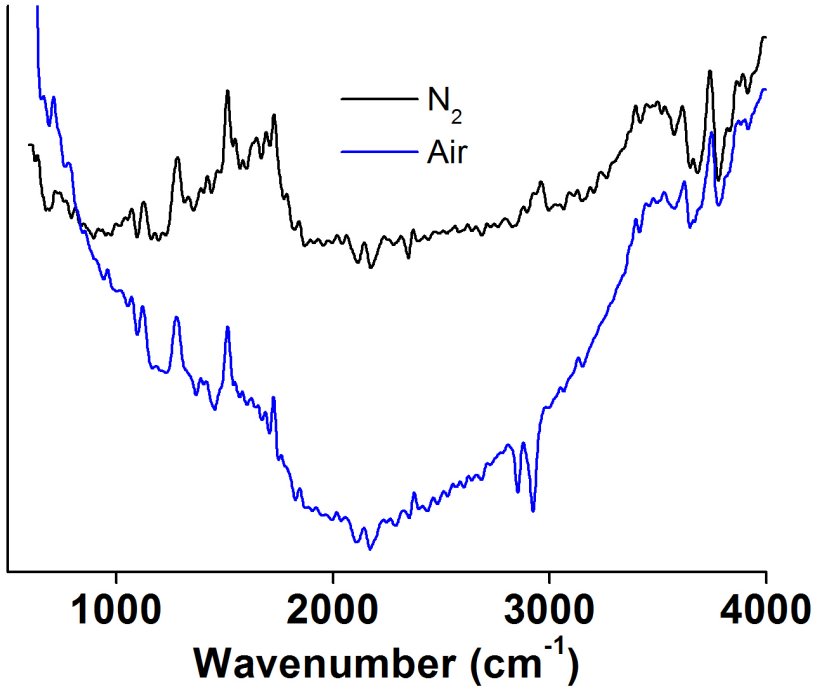

Figure S66: FTIR spectra of Cu and CuO nanoparticles prepared by thermolysis of **(Cu-TBA-2F)** in N_2 and air respectively.

Section 14. Detailed synthesis procedure and characterisation of supported carbon matrix:

The as prepared $[Cu_2(hfbba)_2(3\text{-mepy})_2]\bullet(DMF)_2(3\text{-mepy})$ **(*F*-MOF-4)** was taken in a silica boat and then placed in a tube furnace and heated from room temperature to 900 ◦C under N_2 with a heating rate of 10 ◦C/min to thermolyze the organic species. After reaching the target temperature, the material was cool to room temperature. The final product was a black coloured powder. This powder was used for carbon characterization.

In room temperature graphite has a Raman band due to Brillouin-zone-center phonon at 1578 cm^{-1} (G band) and 1350 cm^{-1} (D band), which are due to a zone-edge phonon that becomes symmetry-allowed in the reduced symmetry environment at the edges of graphite crystals.[28] The Raman bands of graphite are enhanced in intensity with visible excitation by the interaction of electronic (π--π*) transitions with vibrational transitions, such that Raman spectra of submicrometer thicknesses of graphite are easily obtained. Graphite retains its structure of stacked planes of six-membered carbon rings even with domain sizes down to nanometer-scale dimensions, and the Raman spectra of nanocrystalline graphite show broadened bands and enhanced intensity in the D band.[29]

Due to the finite crystal size, an A_g mode of the lattice becomes Raman active. The intensity of this band allows the measurement of *La* in a thin surface layer of any carbon sample. The 1355 cm^{-1} band is attributed to a particle size effect. The ratio of the intensities of 1360 cm^{-1} to 1580 cm^{-1} has been.[31]

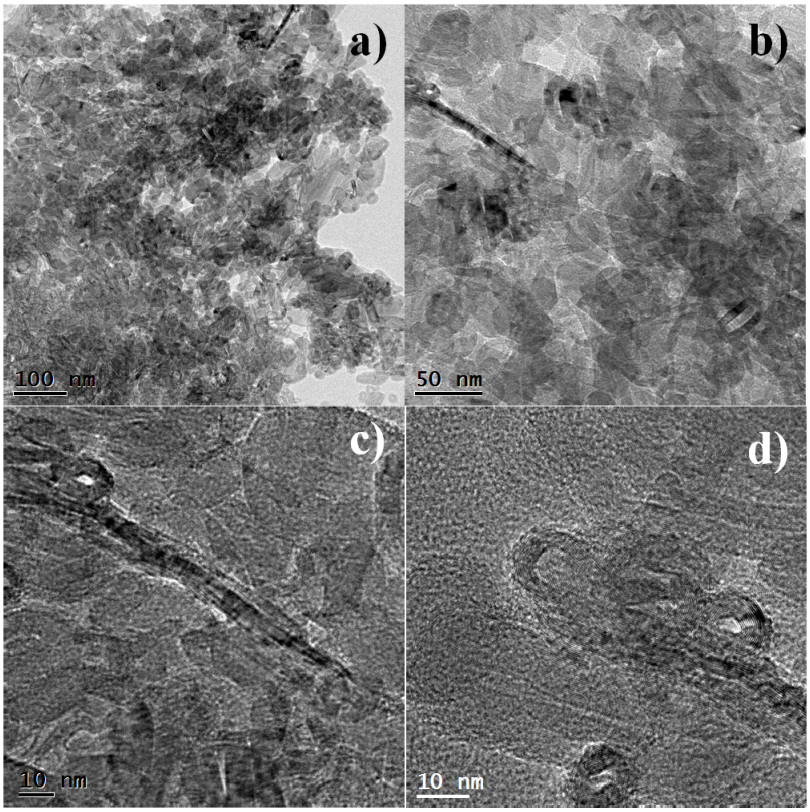

Figure S67: High resolution TEM images of carbon nanofibers matrix formed when thermolysis is carried in N_2.

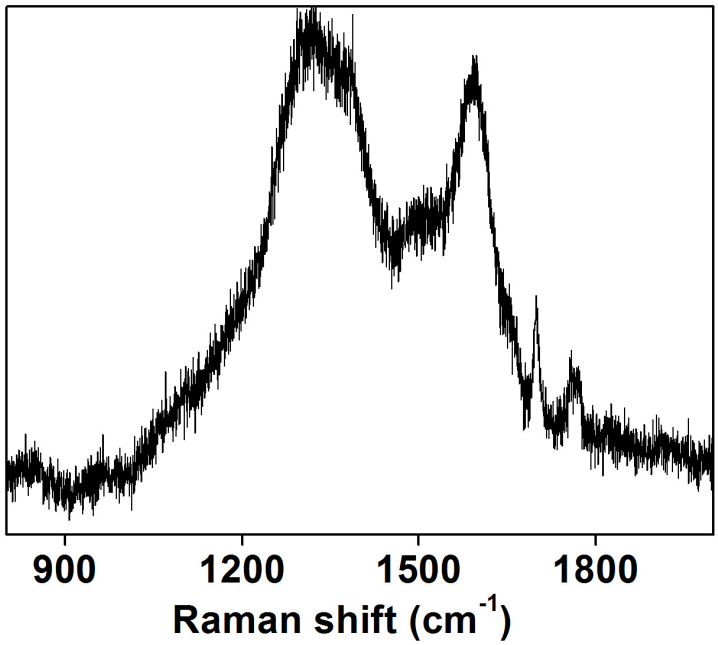

Figure S68: Room temperature Raman spectra of carbon matrix prepared by thermolysis of FMOF-4 in nitrogen**.** Two intense peaks at 1318 and 1593 cm^{-1} shows the carbon matrix is graphite fibres**.**

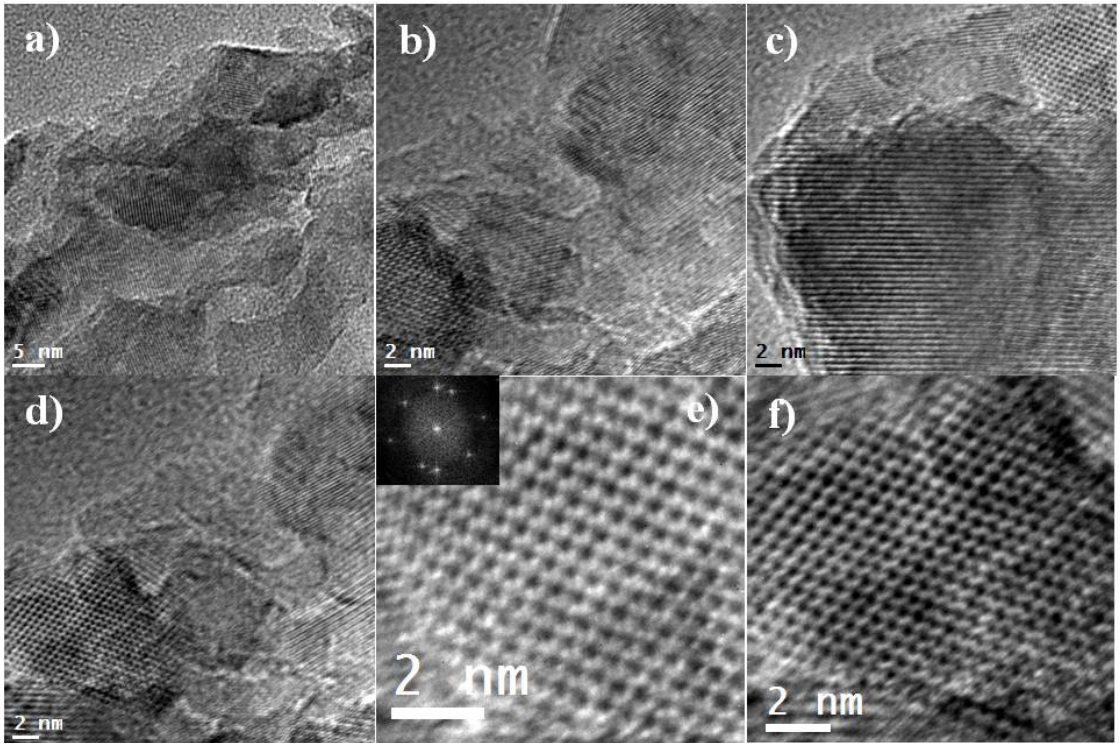

Figure S69: High resolution TEM images of nanocrystalline graphite matrix formed when thermolysis is carried in air.

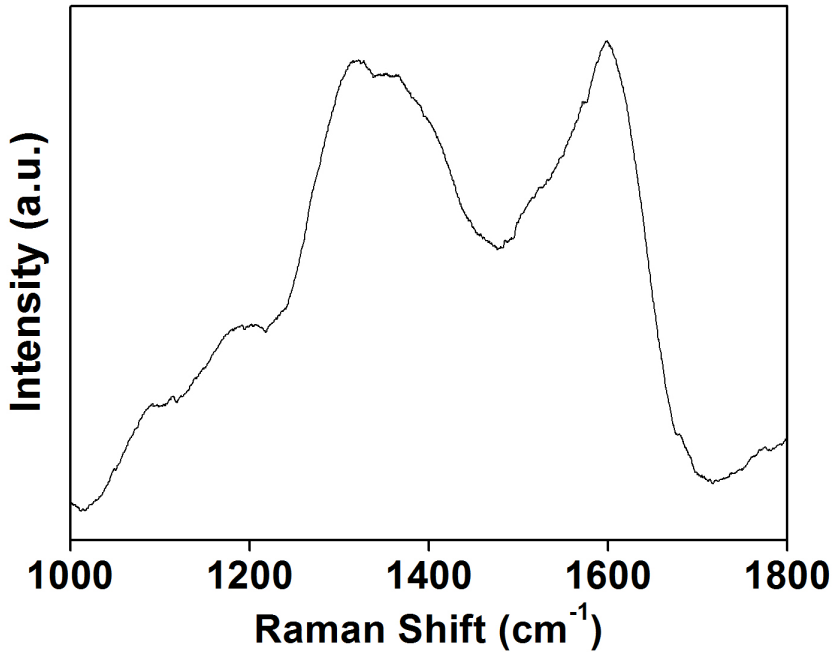

Figure S70: Room temperature Raman spectra of carbon matrix prepared by thermolysis of FMOF-4 in air**.** Two broad humps show the nanocrystalline nature of the carbon.

Section 15. Cyclic Voltametry

All electrochemical studies were performed on an Autolab PGSTAT30 (Eco Chemie) instrument using a conventional three electrode test cell with a 5 mm diameter glassy carbon (GC) electrode coated with the sample as the working electrode (WE), $Hg/HgSO_4$ as the reference electrode (RE) and Pt foil as the counter electrode (CE). The working electrode was prepared as follows. 10 µl of the slurry made by sonicating 5 mg of the material in 1 ml ethanol was drop-coated on glassy carbon electrode. After this, 2µl of 0.01 wt% Nafion diluted with ethanol was coated on the surface of the catalyst layer to yield a uniform thin film. This electrode was then dried in air and was used as the working electrode for all electrochemical studies. An aqueous solution of 0.5 M H_2SO_4 was used as the electrolyte for normal cyclic voltammetric analysis. The CV measurement was taken at a scan rate of 10, 50, 100, 150 and 200 mVs^{-1}.

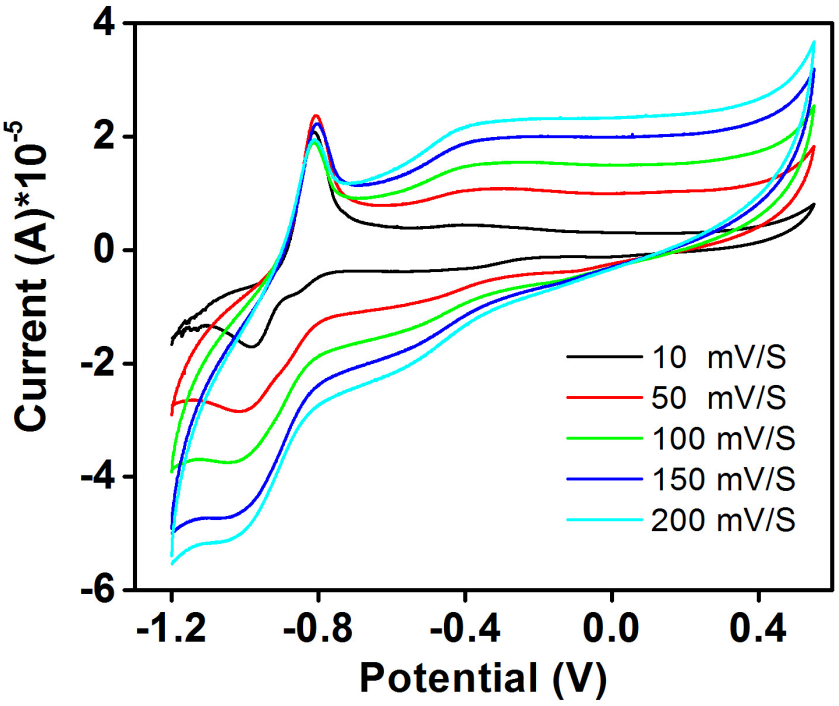

Figure S71: Cyclic voltagram of carbon blended Cu nanoparticles with scan rate of 10-200 mV/s.

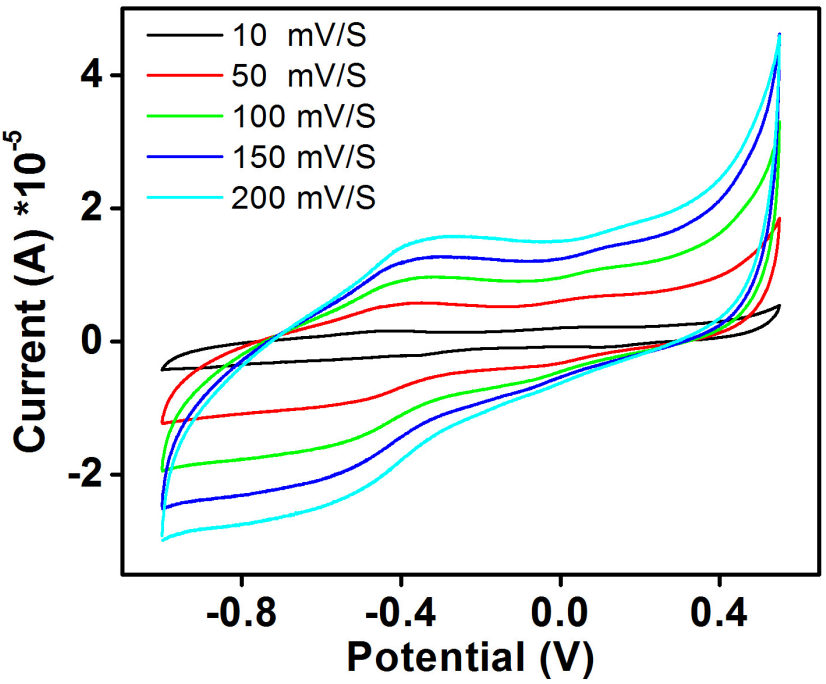

Figure S72: Cyclic voltagram of carbon blended CuO nanoparticles with scan rate of 10-200 mV/s.

Section 16. Role of redox potential

To explore the redox reaction and roles of the redox potential of various cations, we selected the MOFs containing cations with varying level of redox potential to cover a broad range. Similar to the Cu and Co based MOFs, thermolysis of Zn, Mn, Mg and Cd based MOFs (Zn-ADA-1, Mn-H*F*MOF-D, α-Mg-Formate, Cd-ADA-1 and Cd-MOF-1) were done under nitrogen and air environment at 10 °C /min heating rate followed by natural cooling. We found that, these MOFs unlike Cu and Co based MOFs when thermolyzed under nitrogen environment do not produce metal nanoparticles. Rather in both N_2 and air atmosphere it gives respective metal oxide particles embedded in carbon matrix as evidence from PXRD and TEM analysis (Fig. 2 and 3). The analysis of the PXRD pattern of Zn-ADA-1 and α-Mg-Formate thermolyzed in N_2 and air showed the evidence of formation of pure ZnO (wurtzite) and MgO (halite) structure, which could be indexed as per the JCPDS file no. 361451 and

450946 respectively (Fig. 3). The broadness of diffraction peaks of ZnO indicated the formation of 20 nm and 100 nm particles when thermolyzed in N_2 and air respectively.[17] TEM images confirms that ZnO particles have plate like morphology with ~25 nm and ~150 nm in dimension when thermolysis was done in N_2 and air. Like the ZnO (wurtzite) the broadness of diffraction peaks for MgO (halite) indicated the formation of nanosized crystallites of 10 nm size. TEM images shows the particles are nearly spherical in morphology and has size ~15 nm embedded in carbon matrix (Fig. 2, S21, S22, S27). SAED image shows a nice ring pattern that clearly exhibits highly crystalline nature of MgO nanocrystals (Fig. S27d). The analysis of the PXRD pattern of Cd-ADA-1 and Mn-H*F*MOF-D thermolyzed air showed the evidence of formation of pure CdO (cubic rocksalt) and Mn_2O_3 which could be indexed as per the JCPDS file no. 050640 and 411442 (Fig. 3, S30). The crystallite size of CdO and Mn_2O_3 are 50 and 150 nm respectively. SAED image shows nice dot pattern clearly exhibiting highly crystalline nature of Mn_2O_3 nanocrystals (Fig. S34b). The analysis of the PXRD pattern of Mn-H*F*MOF-D thermolyzed in N_2 (Fig. S33 from SI) could not indexed to any Mn and MnO phases. When Cd-MOF-1 was thermolyzed in nitrogen, it produced CdS nanoparticles of ~50 in size and semi spherical shape which was confirmed by PXRD, TEM analysis (Fig. 3 and S37).

Section 17. Effect fluorine in organic backbone of MOFs

The MOFs used as starting materials in the synthesis of Cu and Co nanoparticles are *F*-MOF-4 and Co-H*F*MOF-D, contains fluorine in the organic backbone. To investigate the effect of fluorine atoms present in the framework, to the resulting metal and metal oxide nanoparticle size and morphology, we thermolyzed Cu-TBA-2 and its isostructural fluorinated analogue Cu-TBA-2F. The evidences of formation of Cu nanoparticles were clearly verified by the

PXRD (Fig. S73) when thermolysis was done in N_2. The TEM images reveal that the resulting Cu nanoparticles are almost 'identical' in shape and size (~10-20 nm) for Cu-TBA-2 and Cu-TBA-2F (Fig. S73, S60 and S61). In both cases the particles are nicely and almost identically dispersed in the carbon matrix. These results prove that, fluorine does not play any role towards the particle formation, size and morphology of the resulting metal/metal oxide nanoparticles. It was also observed that both Cu-TBA-2 and CuTBA-2F results in pure CuO phase (like *F*-MOF-4), when thermolysis was done in air (Fig. S62).

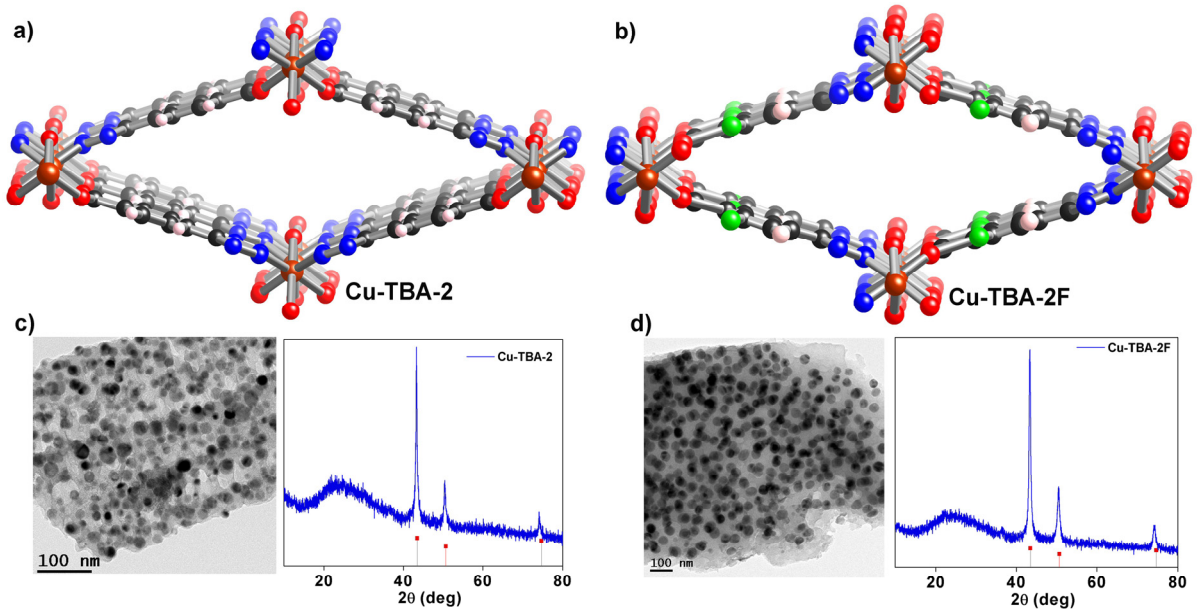

Figure S73. Effect of fluorine atoms present in the MOFs on the formation of metal nanoparticles. Thermolysis of non-fluorinated **Cu-TBA-2** and fluorinated **Cu-TBA-2*F*** resulted into the formation of same morphology Cu nanoparticles. (a) Crystal structure of **Cu-TBA-2**. (b) Crystal structure of **Cu-TBA-2*F***, where fluorine atoms are pointing inside the pores. (c) TEM image of Cu nanoparticles formed by the thermolysis of **Cu-TBA-2** (left), and PXRD pattern of these Cu nanoparticles (right). (d) TEM image of Cu nanoparticles formed by the thermolysis of **Cu-TBA-2*F*** (left), and PXRD pattern of these Cu nanoparticles (right).